Scientific Reports

https://doi.org/10.1038/s41598-026-38306-z

Article in Press

Exosomes derived from bone marrow mesenchymal stem cells facilitate repair of radiation-Induced skin injury by attenuating inflammation and apoptosis

Received: 3 September 2025

Accepted: 29 January 2026

Published online: 02 February 2026

Cite this article as: Wen Y., Song Y., Pan S. *et al.* Exosomes derived from bone marrow mesenchymal stem cells facilitate repair of radiation-Induced skin injury by attenuating inflammation and apoptosis. *Sci Rep* (2026). https://doi.org/10.1038/s41598-026-38306-z

Yuxin Wen, Yiwei Song, Shichao Pan, Na Zhang & Xu Tong

Exosomes Derived from Bone Marrow Mesenchymal Stem Cells Facilitate Repair of Radiation-Induced Skin Injury by Attenuating Inflammation and Apoptosis

Yuxin Wen[1], Yiwei Song[2], Shichao Pan[3], Na Zhang[4], Xu Tong[4,*]

[1] College of Medical Technology, Qiqihar Medical University, Qiqihar 161006, China

[2] The Third Clinical Medical College, Qiqihar Medical University, Qiqihar 161006, China

[3] Department of Radiology, Affiliated Hospital of Jining Medical University, Jining 272000, China

[4] Department of Radiation Oncology, The Third Affiliated Hospital of Qiqihar Medical University, Qiqihar 161000, China

* Corresponding author. E-mail: cn_tongxu@163.com

Abstract

Radiation-induced skin injury (RISI) refers to injury to the skin resulting from exposure to ionizing radiation, for which current treatment options are limited. Exosomes derived from bone marrow mesenchymal stem cells (BMSCs-Exos) have demonstrated significant potential in tissue repair. This study evaluated the healing efficacy of BMSCs-Exos in a rat model of RISI. BMSCs-Exos were isolated and delivered via subcutaneous injection into the RISI. Our findings revealed that BMSCs-Exos reduced the wound area and lowered the radiation injury score, thereby indicating their capacity to facilitate RISI healing. Histological analysis revealed that BMSCs-Exos enhanced epidermal repair and collagen deposition. Immunological assays revealed significantly higher CD31 and α-SMA expression of the BMSCs-Exos treatment group (EXO) than that of the irradiation group (IR), suggesting that BMSCs-Exos promoted angiogenesis. In the EXO group, there was also a downregulation of CD86, Inducible Nitric Oxide Synthase (INOS), Tumor Necrosis Factor-α (TNF-α) and Interleukin-1β (IL-1β) expression, coupled with an upregulation of Macrophage Mannose Receptor 1 (CD206), Arginase-1 (Arg-1), and Interleukin-10 (IL-10) expression, indicating that BMSCs-Exos can induce macrophage polarization towards the M2 phenotype and suppress inflammation. Additionally, BMSCs-Exos decreased the number of TUNEL-positive cells. Western blot analysis of apoptosis-related proteins showed that BMSCs-Exos increased the Bcl-2 expression and reduced Bax expression and promoted phosphorylation of the Akt signaling pathway, which implied suppression of cellular apoptosis. In summary, our findings demonstrate that BMSCs-Exos promote RISI repair by regulating the inflammatory microenvironment, and inhibiting cell apoptosis.

Keywords Radiation-induced skin injury · Exosomes · Bone marrow mesenchymal stem cells ·Macrophage polarization · Inflammation · Apoptosis

Introduction

Radiation-induced skin injury (RISI) stands as a prevalent and severe complication in tumor radiotherapy. Clinical statistics indicate that approximately 85% to 95% of radiotherapy patients undergo varying degrees of skin damage, with clinical manifestations progressing from initial erythema and desquamation to the potential development of chronic ulcers in advanced stages. This not only significantly impacts the treatment outcomes but also markedly diminishes the quality of patients' life [1, 2]. Different from general wounds, the pathogenesis of radiation-induced skin damage is intricate, involving multiple mechanisms, including inflammatory responses, cell apoptosis, and impaired tissue repair. Exposure to high doses of radiation can induce acute skin damage and apoptosis and necrosis of radiation-sensitive cells [3]. Concurrently, macrophages, neutrophils, and eosinophils are recruited to the injury site during the early stages of acute injury. The infiltration of these immune cells promotes the expression of pro-inflammatory cytokines [4]. Through a positive feedback mechanism, pro-inflammatory chemokines and cytokines continuously promote macrophage recruitment and polarization toward the M1 phenotype. The sustained M1 polarization of Macrophages contributes to prolonged inflammation and impaired tissue regeneration [5] , and the microvascular system at the irradiated site becomes disrupted. These factors collectively hinder the regeneration of wound tissues and compromise tissue repair. These characteristics highlight the complexity of RISI, distinguish it from general wounds, and suggest the necessity of developing targeted therapeutic approaches to address its unique healing impairments.

Currently, there are no recognized specific therapies or standard dosing guidelines for RISI, with clinical management primarily reliant on empirical symptomatic supportive treatment [6]. In light of the absence of effective interventions, therapeutic strategies aimed at promoting tissue regeneration have gained increasing attention. Mesenchymal stem cells (MSCs), recognized for their multilineage differentiation capacity and paracrine-mediated regenerative effects, have become a key point of research. Numerous studies have confirmed that MSC transplantation can accelerate the healing of various acute and chronic wounds, improve healing quality, and reduce scar formation [7]. However, clinical application of MSCs-based therapy is associated with several limitations, including

poor survival and low homing rates of transplanted cells at irradiated wound sites, as well as potential risks such as immune rejection, abnormal differentiation, and even tumorigenesis [8, 9]. Subsequent investigations have shown that a significant portion of the therapeutic benefits of MSCs can be mediated by their secreted exosomes. Exosomes, as a cell-free therapy, overcome several limitations of MSCs therapies and are increasingly emerging as a promising strategy in wound healing research [10].

Exosomes are nanosized extracellular vesicles (50-150 nm) secreted by mammalian cells and enriched with lipids, mRNA, and microRNA, which regulate diverse physiological and pathological processes [11, 12]. These vesicles play multiple beneficial roles in promoting wound healing, including stimulating cellular proliferation and migration, promoting angiogenesis, modulating wound inflammation, accelerating re-epithelialization, and reducing scar formation [13, 14]. In myocardial injury models, BMSCs-Exos have been shown to modulate macrophage polarization, thereby reducing inflammation and tissue damage in the heart [15]. Similarly, BMSCs-Exos have also demonstrated significant efficacy in enhancing tissue regeneration and functional recovery in the repair of other wounds, such as burns and diabetic ulcers [16, 17]. The bioactive components carried by BMSCs-Exos can activate relevant signaling pathways to promote cell proliferation, suppress apoptosis, and facilitate general skin wound healing [18]. However, RISI represents a unique type of wound characterized by cytotoxicity, vascular damage, and chronic inflammation, underpinned by more complex pathological mechanisms compared to other types of wounds. Ionizing radiation not only causes acute tissue damage but also triggers persistent chronic inflammation, irreversible microvascular injury, and prolonged oxidative stress, collectively contributing to a significantly impaired healing process. Given the promising prospects of BMSCs-Exos in wound repair, this study proposes and validates the potential of BMSCs-Exos as a therapeutic strategy for RISI. We aim to clarify the functional role of BMSCs-Exos in RISI repair, with particular emphasis on their capacity to regulate inflammatory responses and inhibit the apoptosis pathway, thereby providing new theoretical insights for the treatment of radiation-induced skin injury.

Results

Isolation and Characterization of BMSCs

As shown in Figure 1A, the cells attached to the culture substrate and displayed a spindle-shaped morphology. Multilineage differentiation assays indicated that, following osteogenic induction, distinct calcium nodules were evident upon Alizarin Red staining, which showed an amber color (Figure 1B). Under adipogenic induction conditions, lipid droplets were observed after Oil Red O staining (Figure 1C). Flow cytometry analysis revealed a high expression of mesenchymal stem cell markers CD44 and CD90, along with low expression of hematopoietic lineage

markers CD34 and CD45 (Figure 1D–G). These findings verify the successful isolation of BMSCs from the bone marrow of SD rats.

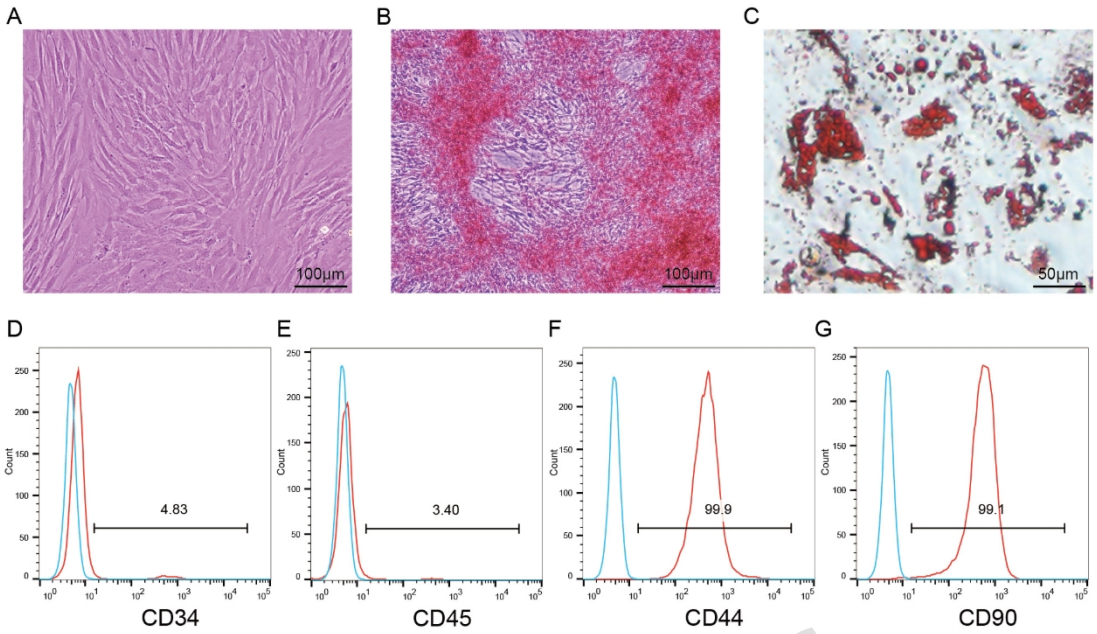

Fig 1. Characterization of BMSCs. Upon observation under an optical microscope: **A** BMSCs exhibited a typical spindle or fusiform shape. Scale bar = 100 μm. **B** Alizarin Red staining demonstrated the presence of calcium nodule deposition. Scale bar = 100 μm. **C** The presence of accumulated lipid droplets was clearly demonstrated through Oil Red O staining. Scale bar = 100 μm. **D–G** Flow cytometry of BMSCs surface markers showing low expression of CD34 (4.83%) and CD45 (3.4%) and pronounced expression of CD44 (99.9%) and CD90 (99.1%).

Isolation and Characterization of BMSCs-Exos

Exosomes were isolated from BMSCs culture supernatant by ultracentrifugation, resulting in an exosome particle concentration of 6.1×10^9 particles/mL, as determined by nanoparticle tracking analysis (NTA). The mean diameter of the exosomes was 144.4 nm (Figure 2B). Transmission electron microscopy (TEM) confirmed that BMSCs-Exos exhibited a cup-shaped or nearly spherical morphology, with a diameter of approximately 128 nm (Figure 2A). Western blot analysis confirmed the presence of exosomal markers CD9, CD63, and TSG101, with no detectable Calnexin expression (Figure 2C), thereby validating the successful isolation of BMSCs-Exos from the culture supernatant.

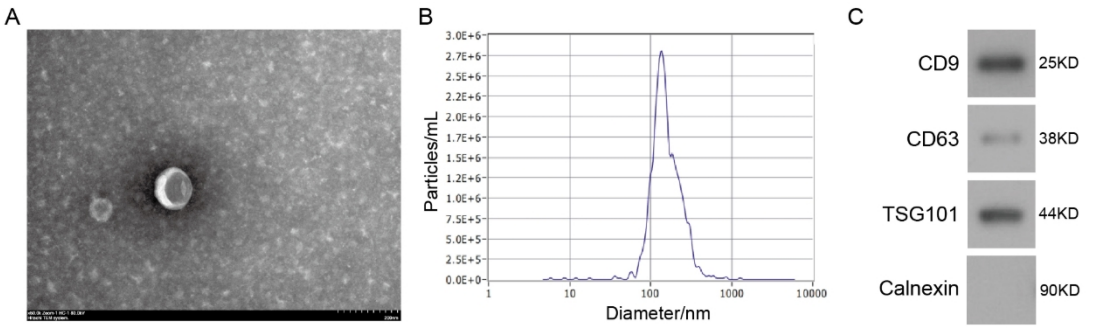

Fig 2. Characterization of BMSCs-Exos. **A** Typical TEM image of BMSCs-Exos, displaying a characteristic cup-shaped morphology. **B** Nanoparticle tracking analysis provided quantitative data on the particle concentration and size distribution of the exosomes. **C** Western blot analysis of CD9, CD63, and TSG101; Calnexin served as a negative control.

BMSCs-Exos are internalized by HDFs and promote fibroblast migration

To determine whether BMSCs-Exos interact with dermal fibroblasts, we first investigated whether BMSCs-Exos can be internalized by human dermal fibroblasts (HDFs). The PKH26-labeled exosomes were internalized by fibroblasts and were clearly visualized by fluorescence confocal microscopy. The red punctate signals were predominantly located in the perinuclear region, indicating successful uptake of exosomes by fibroblasts (Figure 3A). We next evaluated whether BMSCs-Exos influence fibroblast behavior associated with wound repair. Scratch closure test results demonstrated that HDFs treated with BMSCs-Exos (100 μg/mL) displayed enhanced wound closure at 12 h and 24 h (Figure 3B).

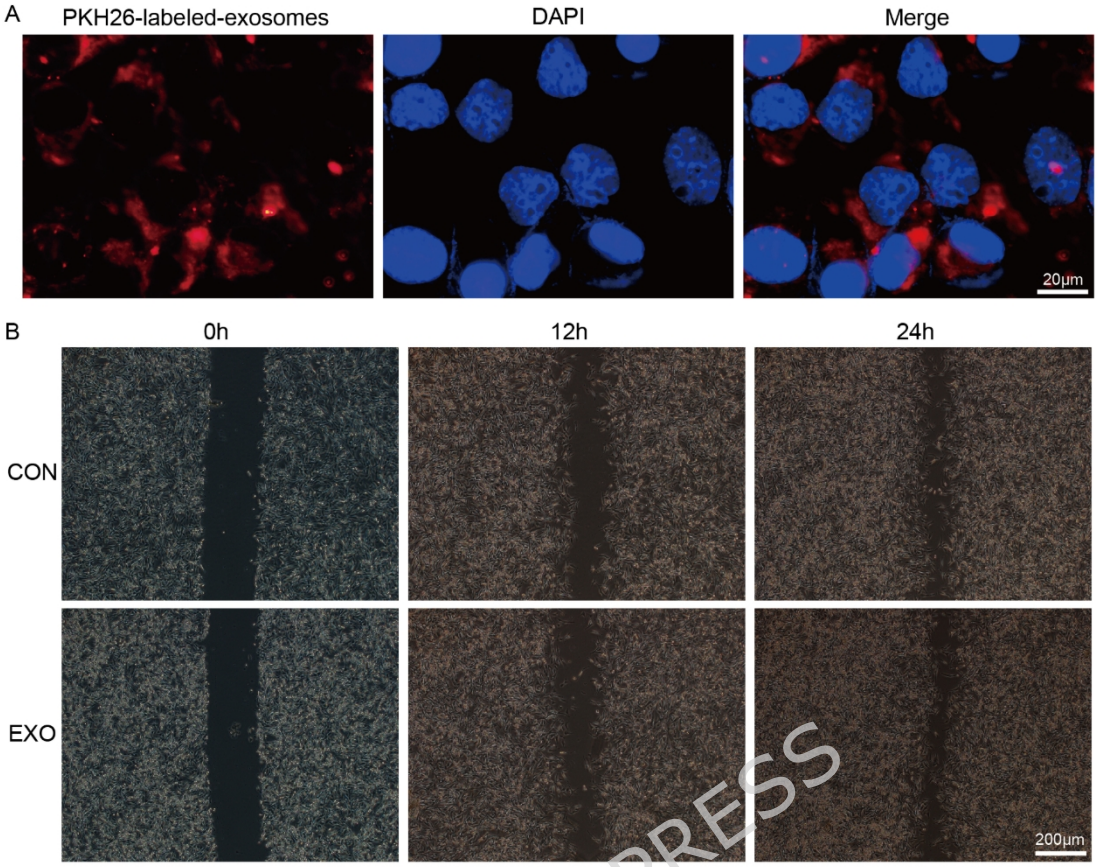

Fig 3. Effects of BMSCs-Exos on HDFs uptake and migration. **A** Confocal fluorescence microscopy illustrated the internalization of PKH 26-labeled exosomes (red) by HDFs. Cell nuclei were subjected to DAPI staining, displaying a blue appearance. **B** Representative images from the scratch wound assay.

Macroscopic Appearance of RISI

To construct the RISI model, the skin of the right hind limb in rats was subjected to a 60-Gy radiation exposure. Treatment commenced on day 10 following radiation exposure, with this time point designated as day 0 of the treatment phase. Wound images were systematically captured and evaluated on days 0, 7, 14, and 21 (Figure 4A). As depicted in Figure 4B, both IR group and EXO group exhibited pronounced radiation-induced skin damage, characterized by extensive erythema, ulceration, and yellow exudates on day 0, thereby confirming the successful establishment of the RISI model. Analysis of the percent of wound areas revealed that, on days 7, 14, and 21, the EXO group demonstrated considerably diminished wound areas when compared with the IR group (Figure 4C). Furthermore, on days 7, 14, and 21, the EXO group showed considerably lower radiation injury scores than the IR group (Figure 4D), indicating that BMSCs-Exos treatment accelerated skin recovery and mitigated radiation-induced damage.

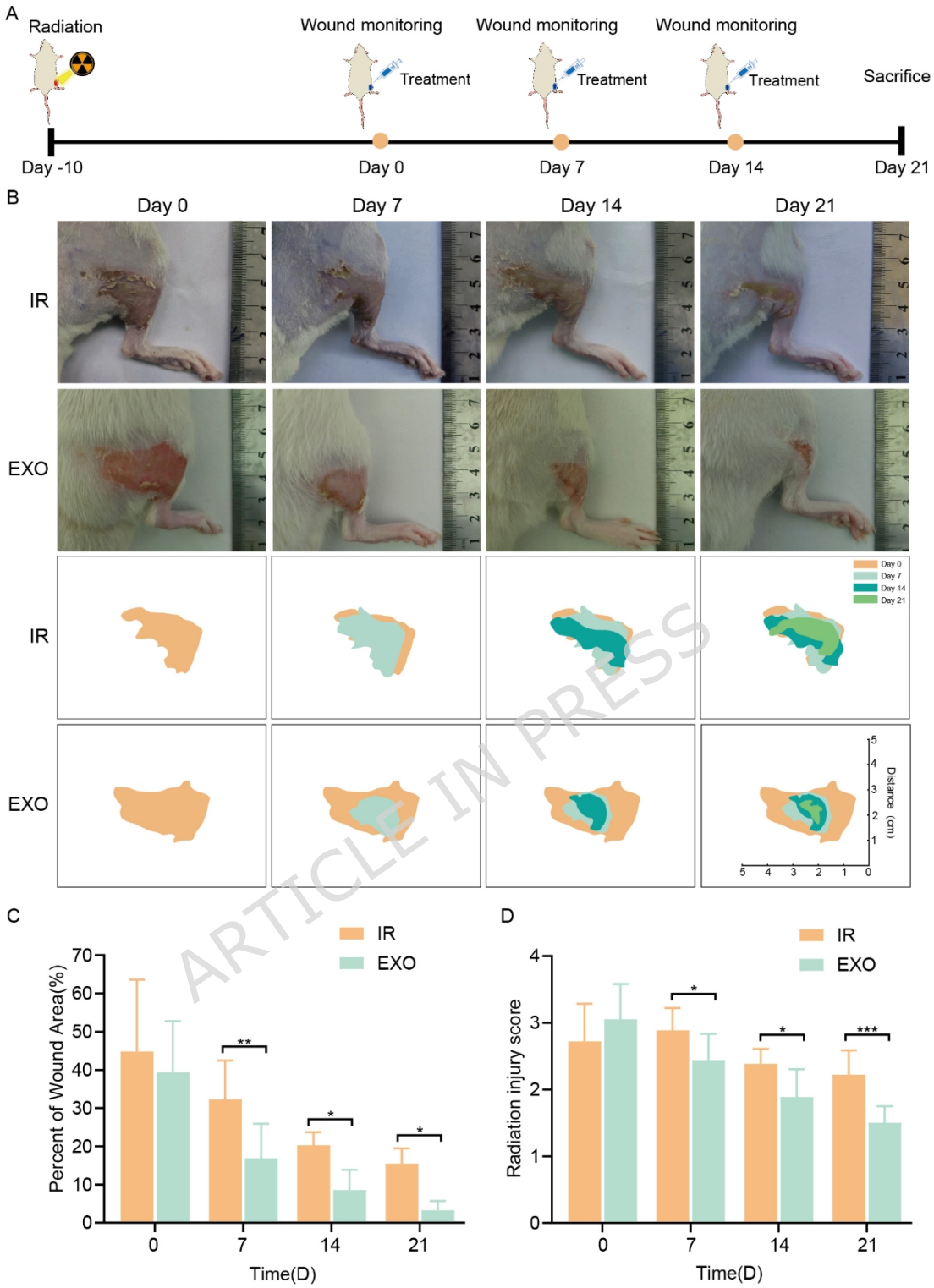

Fig 4. Impact of BMSCs-Exos on the Healing of RISI. **A** Schematic representation outlining the establishment of RISI model and the timeline for exosome treatment administration. **B** Representative photographs of the regenerative progression of RISI and schematic diagrams of wound areas. **C** Quantitative assessment of the percent of wound areas in radiation-induced skin injury across different treatment groups. **D** Radiation injury scoring

system to evaluate the severity of skin damage. Statistical significance: $*P < 0.05$, $**P < 0.01$, $***P < 0.001$.

Histopathological Changes in RISI Treated with BMSCs-Exos

Hematoxylin and Eosin (H&E) and Masson's trichrome staining were carried out to assess histopathological changes in skin tissues. H&E staining revealed that the Control group (CON) displayed an intact skin structure, while the IR group showed epidermal defects, inflammatory cell infiltration, and destruction of skin appendages. In contrast, the EXO group displayed partial epidermal recovery and reduced inflammatory infiltration (Figure 5A). Masson's trichrome staining demonstrated that the CON group possessed a well-organized collagen structure, whereas the IR group exhibited sparse, disorganized collagen fibers. The EXO group showed a significant improvement in collagen fiber organization, resembling the normal skin structure, although the arrangement remained somewhat disordered (Figure 5B). Quantitative assessment of collagen content revealed that the EXO group had elevated collagen levels compared to the IR group, although these levels remained inferior to those detected in the CON group, with statistically significant differences noted (Figure 5C). These findings collectively suggest that BMSCs-Exos promote epidermal repair and collagen synthesis, expediting the regenerative progression in RISI.

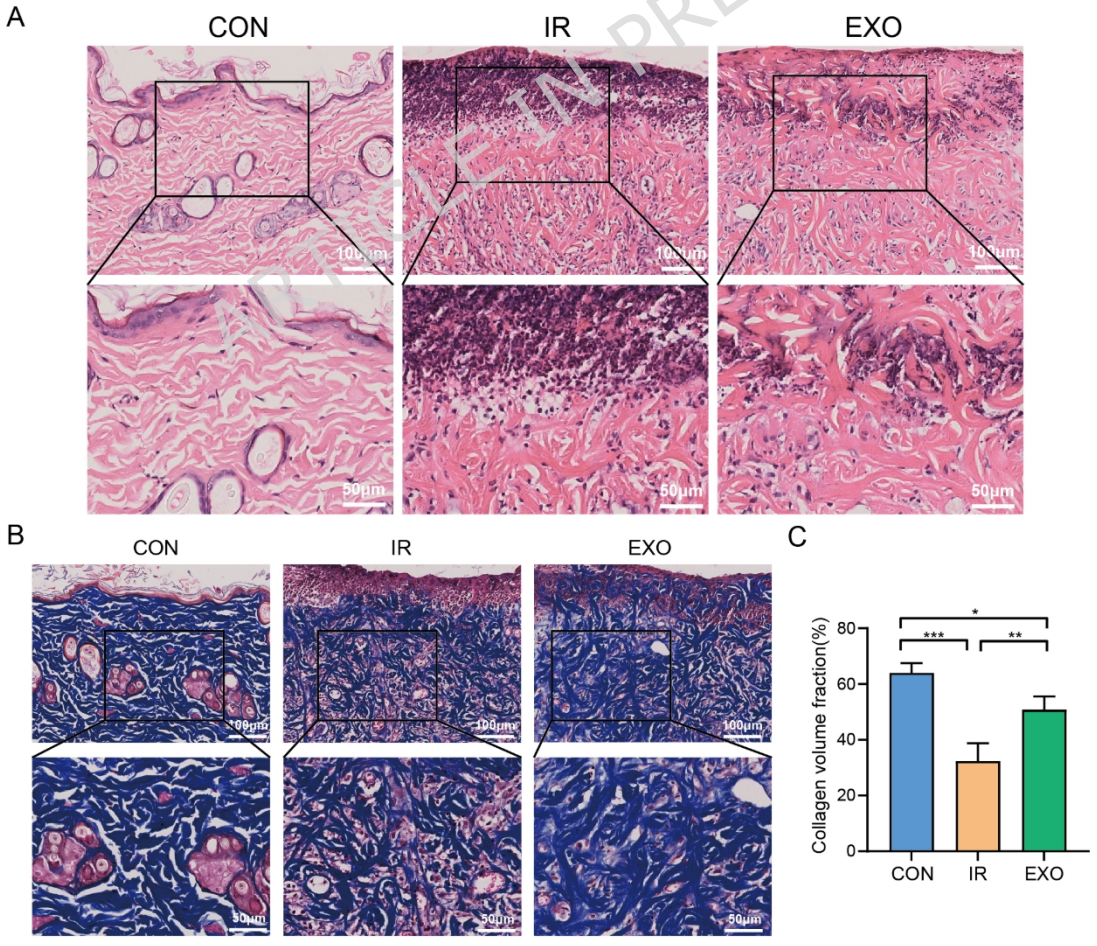

Fig 5. The effect of BMSCs-Exos on radiation-induced skin injury (RISI) and the histological analysis. **A** H&E staining of skin sections. Scale bars: 100 μm. **B** Masson's trichrome-stained skin sections. Scale bars: 100 μm. **C** Measurement of collagen volume fraction (CVF) in skin tissues. The data stand for the mean ± SD, n = 3/per group. *$P < 0.05$, **$P < 0.01$, ***$P < 0.001$. The CON group: Received identical anesthesia and positioning, with no radiation exposure.

Effect of BMSCs-Exos on Angiogenesis in RISI

Immunohistochemical staining was performed to examine the expression of endothelial cell marker CD31 and vascular smooth muscle cell marker α-SMA, to further explore whether BMSCs-Exos promote angiogenesis at the injury site. As shown in Figure 6, the EXO group displayed markedly enhanced neovascularization in comparison to the IR group, as indicated by elevated CD31 expression. Furthermore, the EXO group exhibited a higher density of mature blood vessels, characterized by elevated α-SMA expression. These results suggest that BMSCs-Exos may promote both angiogenesis and vascular maturation, thereby improving tissue perfusion and nutrient supply to optimize the microenvironment conducive to wound healing.

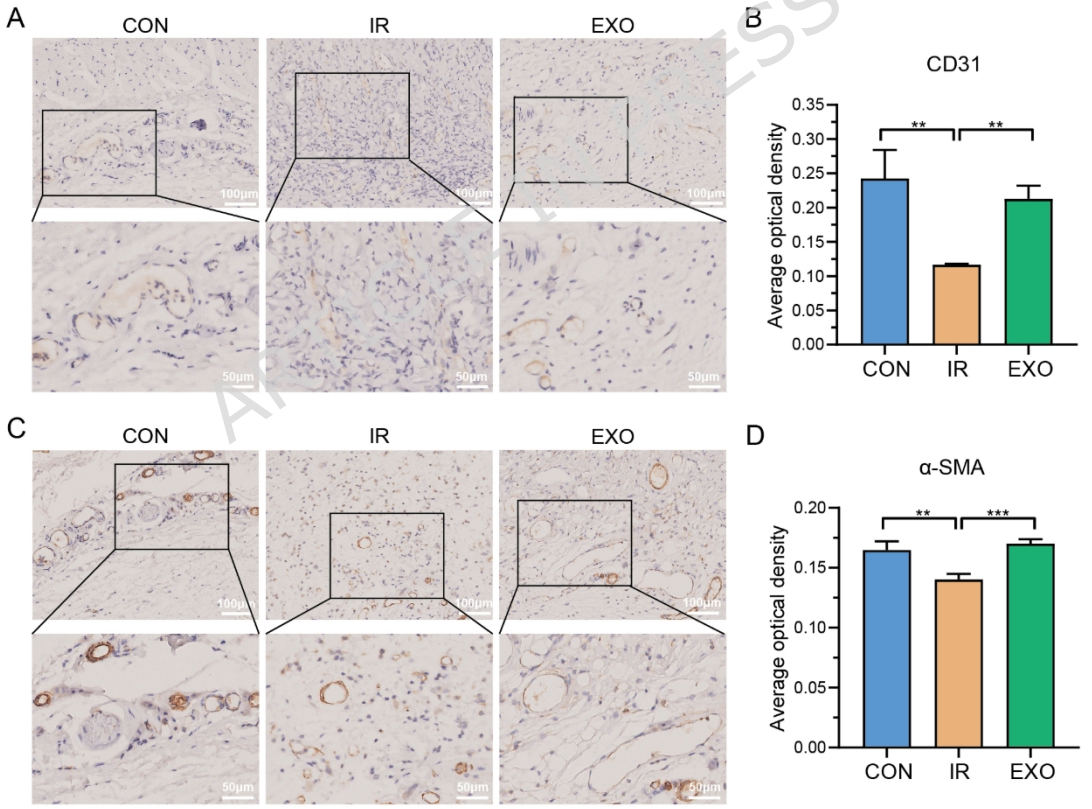

Fig 6. Effect of BMSCs-Exos on Angiogenesis in RISI. **A, C** Immunohistochemical staining of CD31 and α-SMA in radiation-induced skin injury. Scale bar = 100 μm. **B, D** Quantitative assessment of the average optical density of CD31 and α-SMA staining in RISI. Statistical significance: *$P < 0.05$, **$P < 0.01$, ***$P < 0.001$.

Effect of BMSCs-Exos on Inflammation Microenvironment in RISI

To further investigate the impacts of BMSCs-Exos on the inflammatory response in RISI wounds, we examined the expression of key markers: CD86 and CD206 as macrophage phenotype indicators, iNOS and Arg1 as functional markers of M1 and M2 macrophages, respectively, along with the cytokines TNF-α, IL-1β, and IL-10. Immunofluorescence results (Figure 7A–D) revealed that in the IR group, the M1 macrophage marker CD86 was significantly upregulated, whereas the M2 marker CD206 showed only a modest increase, indicating that radiation injury primarily triggers an M1-dominant inflammatory response. After BMSCs-Exos intervention, a notable decrease in CD86 expression was observed, accompanied by a significant upregulation of CD206. Western blot analysis (Figure 7E–G) further corroborated these findings, revealing a reduction in iNOS (an M1 pro-inflammatory factor) expression and a concurrent increase in Arg-1 (an M2 repair factor) levels in the EXO group, suggesting that BMSCs-Exos promote macrophage polarization toward the M2 phenotype. Figure 8 illustrates that there was an elevation in TNF-α and IL-1β expression in the IR group, alongside a moderate increase in IL-10, suggesting an initial attempt by the body to mount an anti-inflammatory response following radiation damage. BMSCs-Exos treatment further inhibited the expression of TNF-α and IL-1β, while significantly boosting IL-10 secretion, thereby amplifying anti-inflammatory effects. These findings suggest that BMSCs-Exos may modulate the inflammatory microenvironment by promoting M2 macrophage polarization and effectively mitigate radiation-induced inflammation.

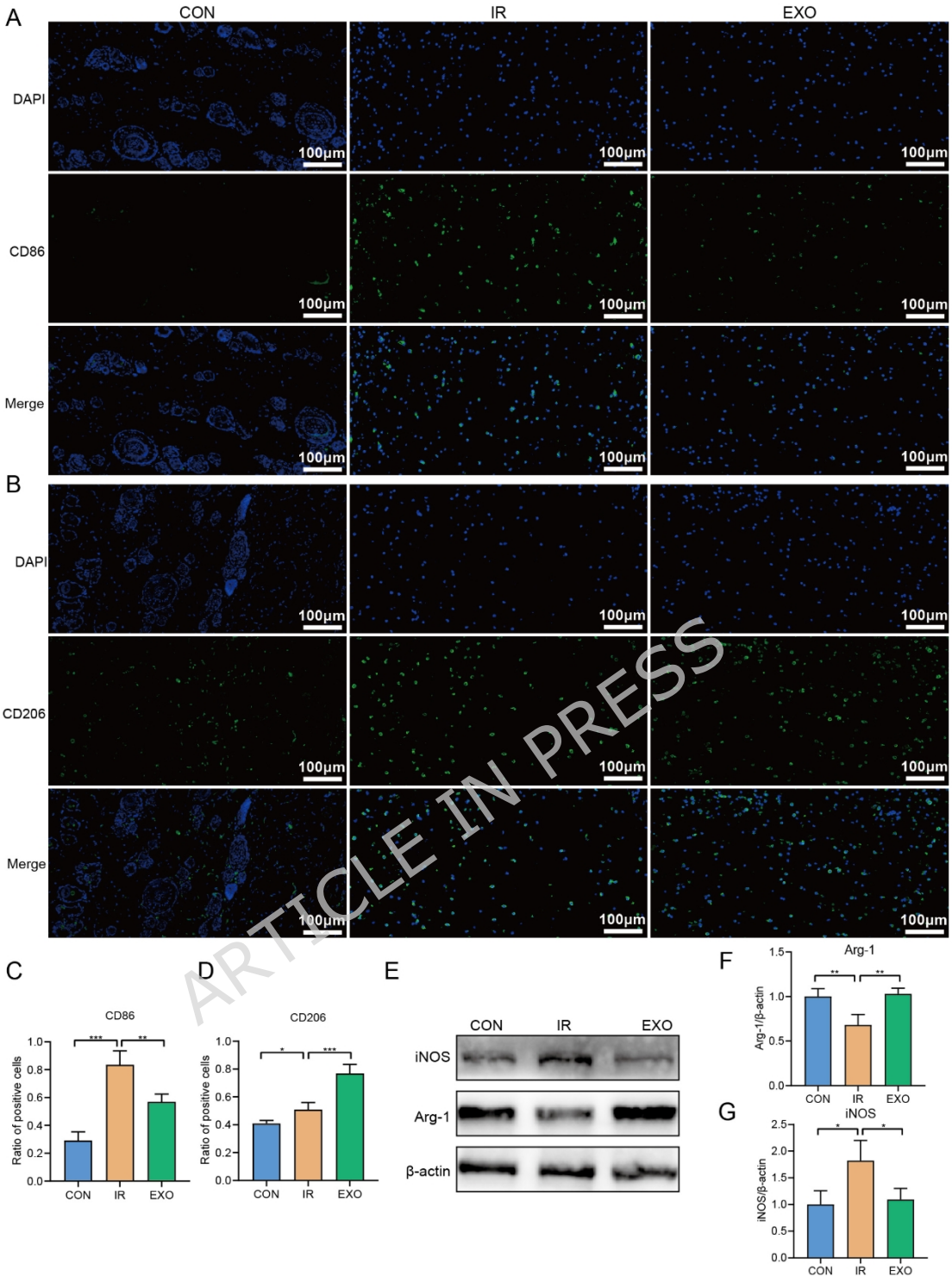

Fig 7. Effect of BMSCs-Exos on Macrophage Polarization in Radiation-Induced Skin Injury. **A, B** Immunofluorescence staining for CD86 and CD206. Scale bar = 100 μm. **C** Statistical analysis of the proportion of CD86-positive cells. **D** Statistical analysis of the proportion of CD206-positive cells. **E–G** Western blot analysis of macrophage phenotype markers iNOS and Arg-1, normalized to β-actin. Statistical significance: $^{*}P < 0.05$, $^{**}P < 0.01$, $^{***}P < 0.001$.

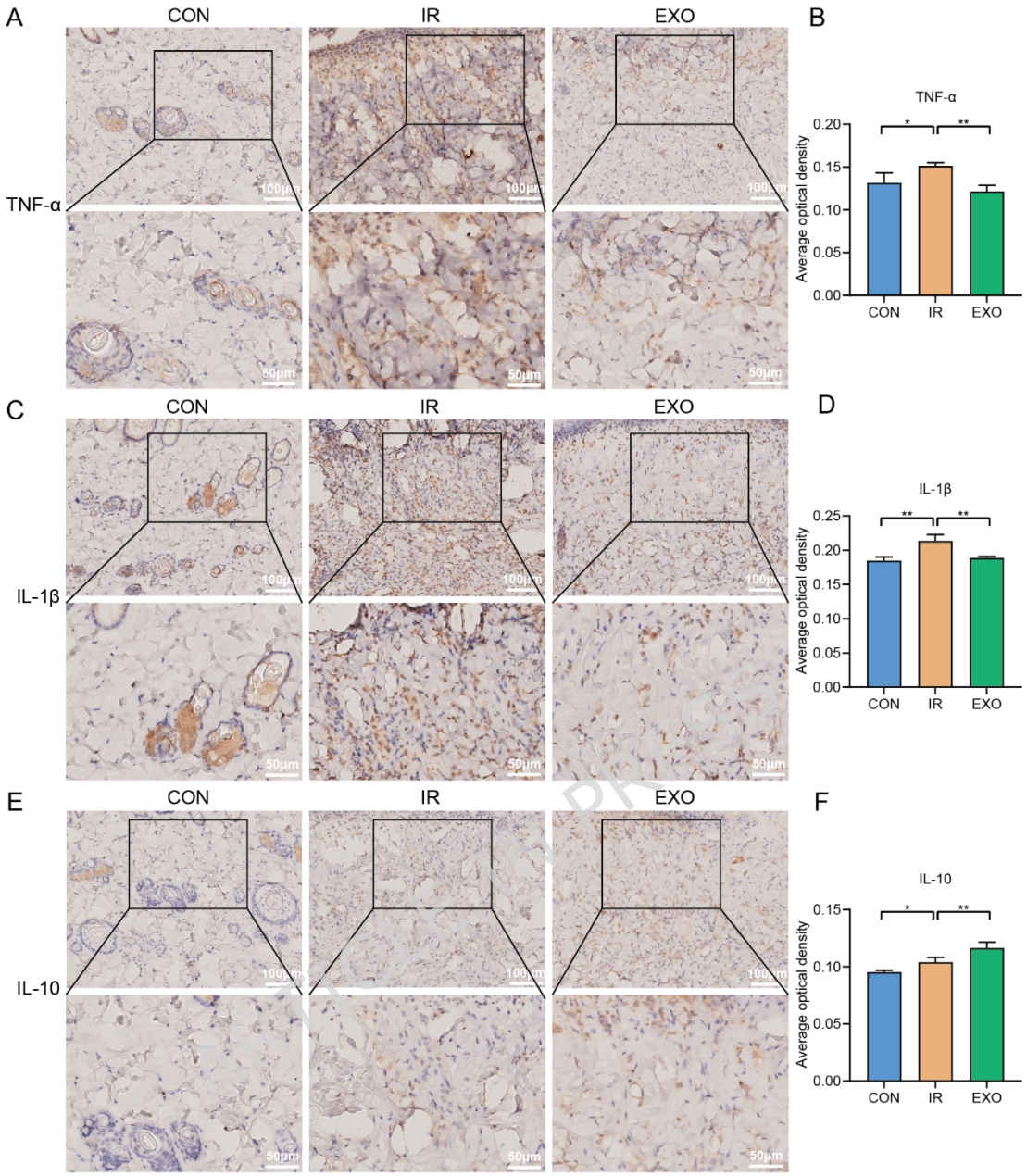

Fig 8. Effect of BMSCs-Exos on Inflammatory Mediators in Radiation-Induced Skin Injury. **A, C, E** Immunohistochemical staining for TNF-α, IL-1β, and IL-10 in radiation-induced skin tissue. Scale bar = 100 μm. Average optical density analysis of **B** TNF-α, D IL-1β, and **F** IL-10 expression in skin tissue. Statistical significance: $*P < 0.05$, $**P < 0.01$, $***P < 0.001$.

Effect of BMSCs-Exos on Reducing Cell Apoptosis in RISI

To study the influence of BMSCs-Exos on apoptosis in RISI, we performed TUNEL staining and Western blotting to analyze the expression of the apoptosis-related proteins Bcl-2 and Bax. TUNEL staining (Figure 9A, B) revealed minimal apoptosis in the CON group, whereas the IR group exhibited a significant elevation in apoptotic cells. Conversely, the EXO group showed a notable reduction in apoptotic cells. As shown in Western blot results (Figure 9C–E), the pro-apoptotic

protein Bax levels decreased while the anti-apoptotic protein Bcl-2 levels increased in the EXO group, suggesting that BMSCs-Exos possess the ability to inhibit apoptosis in RISI.

To elucidate the anti-apoptotic mechanism of BMSCs-Exos, we conducted a comprehensive assessment of the expression intensities of pivotal proteins within the Akt signaling pathway. Our results (Figure 9F, G) showed that after BMSCs-Exos treatment, there was a significant upregulation in the phosphorylation levels, accompanied by an increased *p*-Akt/Akt ratio. The observation suggests that the Akt signaling pathway may play an important role in the anti-apoptotic effects mediated by BMSCs-Exos.

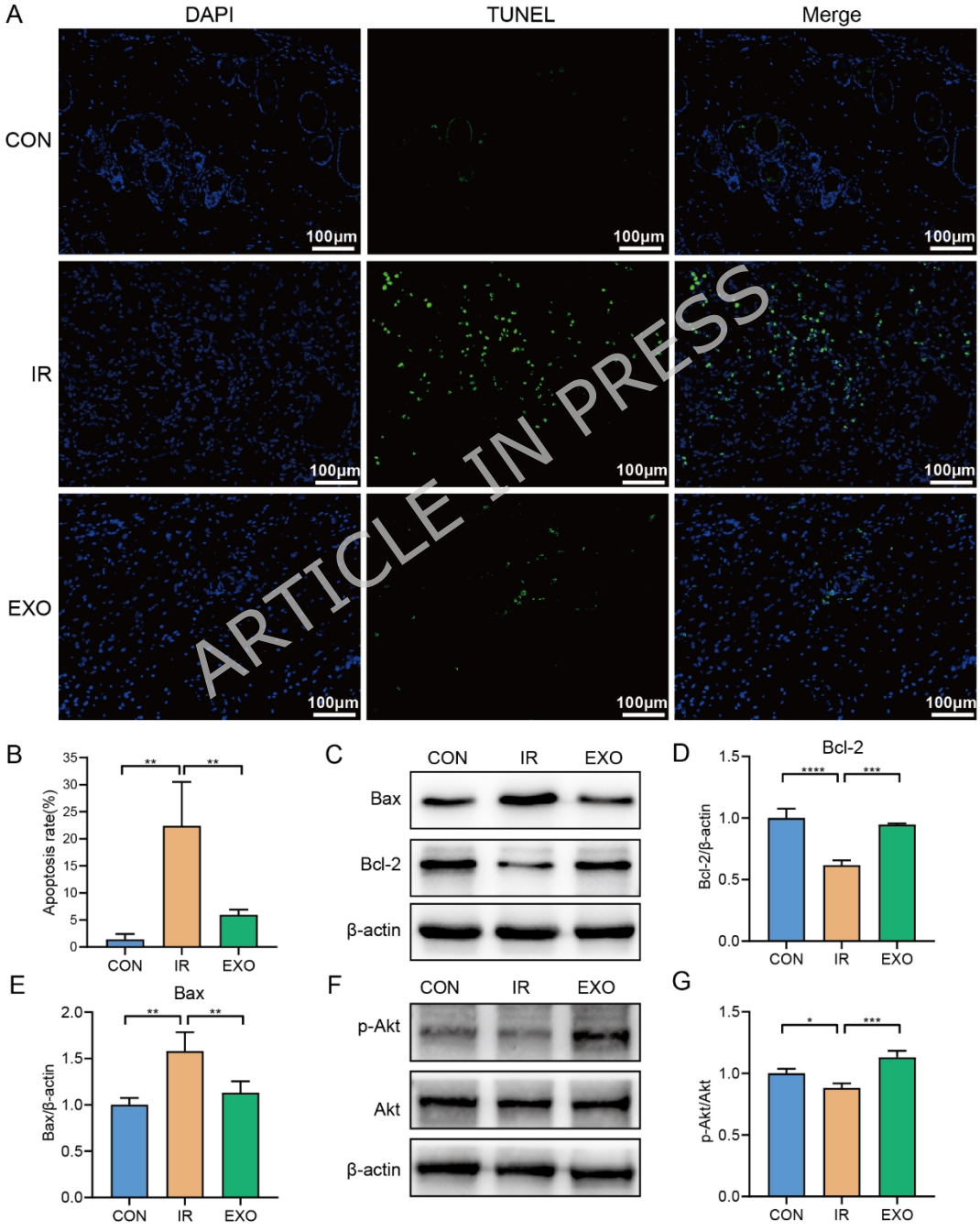

Fig 9. Effect of BMSCs-Exos on Cell Apoptosis in RISI. **A, B** TUNEL staining and positive rate analysis of the RISI region. Scale bar = 100 μm. **C–E** Western blot analysis showing Bax and Bcl-2 protein expression, with densitometric quantification normalized to *β*-actin. **F, G** Western blot analysis and quantitative optical density analysis of the Akt signaling pathway, including *p*-Akt/Akt proteins, normalized to *β*-actin. Statistical significance: $*P < 0.05$, $**P < 0.01$, $***P < 0.001$.

Discussion

RISI is a distinct type of tissue injury induced by ionizing radiation, which differs from conventional wounds such as burns and trauma. RISI is characterized by delayed onset, progressive nature, and poor healing. Clinically, it progresses from early erythema and desquamation to late-stage ulceration, fibrosis, and even necrosis, with the healing process typically being slow and prone to secondary infections [19, 20]. The healing of general wounds usually proceeds through four stages: hemostasis, inflammation, proliferation, and remodeling. These processes rely on cellular regeneration and the coordinated immune and vascular responses [21]. However, the healing process of RISI is severely disrupted by apoptosis, microvascular damage, and persistent inflammation. Ionizing radiation causes direct DNA damage to basal keratinocytes and endothelial cells, significantly increasing the generation of reactive oxygen species (ROS), which triggers apoptosis and the release of pro-inflammatory cytokines (such as TNF-α, IL-1β, and IL-6). This leads to a prolonged inflammatory state and disrupts the endothelial system of microvessels, causing impaired blood supply. These pathological features make the healing process of RISI more complex and prolonged compared to general wounds [22, 23].

In recent years, mesenchymal stem cell-derived exosomes (MSCs-Exos) have attracted significant attention for their promising potential in immune regulation and tissue repair, emerging as a focal point of research in wound healing [24-26]. In this study, we isolated and prepared BMSCs-Exos and administered them to treat RISI. Treatment with BMSCs-Exos significantly promoted wound healing, evidenced by a notable decrease in wound area and radiation injury scores in the EXO group relative to the IR group. Histological analysis revealed that the epidermis in the IR group was necrotic, skin appendages were absent, and collagen fibers were sparse and disorganized. In contrast, following BMSCs-Exos therapy, partial epidermal recovery, increased collagen deposition, and improved tissue structure. Experimental evidence supports that BMSCs-Exos serve as key regulators in the healing of RISI, likely attributable to their ability to promote angiogenesis, as well as regulate the inflammatory microenvironment and reduce apoptosis, thereby providing a favourable repair microenvironment for tissue regeneration and healing.

Adequate local blood circulation is paramount for effective skin repair. However, ionizing radiation disrupts the skin’s microcirculation network, causing angiogenic impairment that limits the supply of oxygen and nutrients, thereby

significantly hindering the wound repair process [27, 28]. Earlier research has indicated that BMSCs-Exos contribute to promoting the formation of functional vascular networks by upregulating the expression of vascular endothelial growth factor A (VEGFA) and platelet endothelial cell adhesion molecule (CD31), thus accelerating tissue repair [14]. Our study showed that BMSCs-Exos treatment significantly increased CD31 and α-SMA expression compared with the IR group, suggesting that exosomes not only promote the formation of new capillaries but also enhance the recruitment of vascular smooth muscle cells, further facilitating vascular maturation. The enhanced angiogenesis improved the local ischemic microenvironment, providing the necessary nutritional support crucial for wound repair. Furthermore, in this study, we observed that BMSCs-Exos promoted collagen accumulation and increased α-SMA expression, BMSCs-Exos can enter the cytoplasm of fibroblasts and promote migration, suggesting that BMSCs-Exos may induce or activate skin fibroblasts, thereby facilitating collagen deposition and phenotypic changes. Studies have shown that bioactive molecules from exosomes can mediate intercellular communication, regulating gene expression and signaling pathways in target cells. BMSCs-Exos activate fibroblasts via the miR-144-3p/miR-23b-3p-PTEN-PI3K/Akt axis, promoting proliferation, migration, and collagen synthesis [29]. In diabetic wound models, lncRNA H19 in BMSCs-Exos transfers to fibroblasts to aid wound healing [30]. BMSCs-Exos also regulate the TGF-β/Smad pathway to stimulate fibroblast activity [31]. Fibroblasts play a crucial role in collagen synthesis and wound healing. BMSCs-Exos may promote RISI healing through similar mechanisms. Future work will focus on better understanding the mechanisms through which BMSCs-Exos regulate the function of radiation-exposed skin fibroblasts, which is essential for enhancing the repair of RISI and supporting the clinical use of BMSCs-Exos.

While angiogenesis plays a crucial role in enhancing nutrient delivery to support tissue repair, the regulation of the inflammatory microenvironment is equally vital. As documented in the literature, the delayed healing of RISI is strongly associated with sustained activation of a pathological inflammatory microenvironment [22, 32]. Macrophages play a key role in inflammation and tissue repair [33, 34]. M1 macrophages secrete pro-inflammatory cytokines, including TNF-α and IL-1β, which perpetuate the inflammatory response, whereas M2 macrophages produce anti-inflammatory cytokines like IL-10, promoting tissue regeneration and repair [5, 35]. MSCs-Exos possess significant promise in modulating the inflammatory microenvironment [36-38]. Our study suggests that BMSCs-Exos may influence macrophage polarization and help mitigate radiation-induced inflammation. These results are consistent with previous studies, reinforcing the notion that BMSCs-Exos alleviate inflammation by regulating macrophage polarization [39]. The shift toward the M2 phenotype may help mitigate excessive inflammation and establish a microenvironment conducive to tissue repair. BMSCs-Exos carrying miR-125a have been shown to promote M2 polarization by downregulating IRF5 [40], while exosomal miR-124-3p enhances

M2 polarization through targeting Ern1 [41]. Radiation-induced damage affects cellular function through complex biological mechanisms, where exosomes, as carriers of bioactive molecules, may regulate intracellular signaling pathways in macrophages by transferring miRNAs, proteins, lipids, and other molecules. In the complex biological context of radiation induced damage by radiation therapy, Prospective research would further explore the key miRNAs within BMSCs-Exos that regulate radiation damage repair, validate their role in radiation-damaged cells, and investigate their potential repair mechanisms, aiming to provide new targeted strategies for the treatment of radiation-induced damage.

Apart from modulating inflammation, reducing cell apoptosis represents another critical mechanism for mitigating radiation-induced skin damage [42]. Our findings demonstrated that treatment with BMSCs-Exos significantly inhibited radiation-induced apoptosis in skin cells, accompanied by reduced Bax expression and increased Bcl-2 expression. Furthermore, we observed an increase in the p-Akt/Akt ratio, suggesting that Akt signaling pathway activation may play a role in reducing apoptosis. This activation enhances cell survival and promotes tissue repair. The Akt pathway, an important regulatory axis in cell survival and anti-apoptosis, phosphorylates downstream effectors such as Bad, GSK-3β, and Caspase-9, thereby blocking mitochondrial pathway-mediated apoptosis and enhancing cell resistance to radiation-induced stress [43]. Notably, exosomes are enriched with miRNAs, which could potentially activate the PI3K/Akt pathway, either directly or indirectly, thus exerting strong anti-apoptotic and tissue regenerative effects [44]. Based on these observations, we hypothesize that the interaction between exosomes, miRNAs, and the Akt pathway may contribute to the efficacy of BMSCs-Exos in radiation damage repair. However, further studies are needed to directly profile the exosomal cargo and functionally test this hypothesis.

Although the results of this study support the potential of BMSCs-Exos in the treatment of RISI, certain limitations still exist. First, this study used a single high radiation dose to induce RISI. While this ensures consistency in the injury model, the radiation doses received by different patients during clinical radiotherapy vary, leading to differences in the severity of radiation-induced skin toxicity. The choice of a single high dose may limit the broader applicability of the findings. Future studies could consider validating the results using a range of radiation doses to enhance the clinical relevance of the findings. Second, although this study provides preliminary evidence for the efficacy of BMSCs-Exos, the specific bioactive molecules within the exosomes have not been thoroughly analyzed, and the direct interactions between exosomes and target cells remain to be further explored. Future research could incorporate in vitro cell models as well as in vivo tracking experiments of exosomes, utilizing techniques such as mass spectrometry and miRNA profiling for a more detailed analysis of the bioactive molecules within exosomes. Additionally, using Akt inhibitors or miRNA knockdown experiments to

validate the specific signaling pathways of exosomes will further elucidate their mechanisms in the repair process.

Materials and Methods

Experimental Animals

In this study, a total of 34 Sprague-Dawley (SD) rats were utilized, comprising 30 healthy adults (10 weeks, 300–350 g), along with 4 juveniles aged 4 weeks and weighing 70–80 g. Animals were sourced from Beijing Vital River Laboratory Animal Technology Co., Ltd. (SYXK [Beijing] 2022-0052). Experimental animals were housed with precisely regulated conditions in a consistently maintained temperature (22 ± 2 °C), relative humidity (50% to 60%), and a 12-hour light/dark cycle. After a 7-day acclimation period, during which animals had unrestricted access to food and water, experimental procedures were initiated. This study was approved by the Animal Ethics Committee of Qiqihar Medical University (QMU-AECC-2024-7). All procedures were performed in strict accordance with the ARRIVE guidelines, and all methods were carried out in accordance with relevant guidelines and regulations.

Isolation, Cultivation, and Characterization of BMSCs

We isolated BMSCs from 4-week-old Sprague-Dawley (SD) rats via whole bone marrow adherence. Cells were incubated in Dulbecco's Modified Eagle Medium/Nutrient Mixture F-12 (DMEM/F12) complete medium supplemented with 10% fetal bovine serum (FBS) and 1% penicillin-streptomycin at 37 °C in a humidified incubator containing 5% CO_2. Cells were passaged sequentially until the third passage (P3). To evaluate their multipotent differentiation capacity, the cells were induced to undergo adipogenic and osteogenic differentiation using standard protocols [45]. Flow cytometry was employed to precisely determine the cell surface marker profile. Briefly, the cell suspension was incubated with fluorochrome-conjugated antibodies against CD34, CD45, CD90, and CD44. Expression intensities of these markers were precisely determined by employing a flow cytometer (Luminex, Austin, Texas, USA).

Characterization of BMSCs-Exos

To isolate BMSC-Exos, the supernatant from BMSCs was collected and centrifuged at 10,000 g for 30 minutes to remove debris. The clarified supernatant was then transferred to a new centrifuge tube and concentrated using a 100 kDa ultrafiltration membrane by centrifugation at 3,500 g for 15 minutes, followed by filtration through a 0.22 μm membrane. The filtrate was transferred to an ultracentrifuge tube and centrifuged at 120,000 g for 90 minutes at 4 °C (Beckman Coulter, Optima XE-100). The supernatant was discarded, and the exosomes were resuspended in PBS. The protein concentration of the exosomes was determined using a bicinchoninic acid (BCA) protein assay kit (Beyotime, Shanghai, China),

and the exosomes were stored at −80 °C for future experiments. The morphology of the isolated exosomes was characterized by transmission electron microscopy (TEM; Hitachi High-Tech Corporation, Tokyo, Japan), and nanoparticle tracking analysis (NTA; Particle Metrix GmbH, Meerbusch, Germany) was used to determine the size distribution and concentration of the exosomes. Western blot analysis was conducted to determine expression of exosomal markers CD9, CD63, and TSG101, while Calnexin, an endoplasmic reticulum protein, served as a negative control to exclude cellular contamination.

Internalization of BMSCs-Exos by HDFs

To investigate exosomal uptake and internalization, BMSC-Exos were labeled with the fluorescent dye PKH26. Human dermal fibroblasts (HDFs) were acquired from Procell (Wuhan, China) and were cultured in DMEM supplemented with 10% FBS and 1% penicillin-streptomycin. HDFs were seeded in 24 well plates and co-cultured with the labeled exosomes for 12 hours at 37 °C. After incubation, the cells were washed with PBS to remove any uninternalized exosomes, fixed in 4% paraformaldehyde, and counterstained with DAPI to visualize cell nuclei. The internalization of labeled exosomes was visualized employing a fluorescence microscope.

HDFs Scratch Assay

The HDFs were seeded in 6-well plates and when they reached a confluence of 80%, scratch wounds were made using a 200 µL micropipette tip. After washing each well twice with PBS, basal DMEM containing BMSCs-Exos at a final concentration 100 µg/mL was added to each well. Wound closure progression was observed and photographed at 0 h, 12 h, and 24 h using an inverted microscope at predefined positions.

Establishment of RISI Model

Following weighing, the rats underwent anesthesia induction through intraperitoneal administration of 1% pentobarbital sodium (30 mg/kg) and were randomly assigned to three groups (n = 10 per group): the Control group (CON), Irradiation group (IR), and BMSCs-Exos treatment group (EXO). Prior to the irradiation, the right thigh of each rat was shaved using an electric hair clipper and treated with a depilatory agent to ensure uniform exposure. The rats were then positioned prone and secured on a custom-built radiation platform. For the IR and EXO groups, a one-time exposure of 60 Gy of radiation was administered to the skin of the right thigh using a linear accelerator under the following parameters: a radiation field size of 3.5 cm × 3.5 cm, source-to-skin distance (SSD) of 100 cm, and dose rate of 999 cGy/min. To ensure dose uniformity, the irradiated area was covered with a 1 cm-thick tissue-equivalent compensating membrane, while adjacent non-irradiated areas were shielded with lead blocks. The CON group underwent identical anesthesia and positioning procedures but received no

radiation exposure. At the end of the experiment, SD rats were euthanized by intraperitoneal injection of 1% pentobarbital sodium at a dose of 200 mg/kg.

Treatment Protocol and Skin Injury Evaluation

After radiation exposure, all rats were subjected to continuous monitoring. The onset of pronounced erythema at the irradiated site was designated as Day 0 (D0) of treatment, marking the initiation of therapeutic interventions. Rats in the EXO group received a subcutaneous injection of 200 μL BMSCs-Exos (100 μg/mL) directly at the radiation-exposed area. The IR group was administered an equal volume of saline through subcutaneous injection, while the CON group remained untreated. The regimen involved 3 injections, each spaced 7 days apart. Wound progression was documented photographically on D0, D7, D14, and D21, with wound areas measured using ImageJ software. RISI was evaluated using the scoring system developed by Douglas and Fowler [46]. The percent of wound area was calculated by employing the given formula:

$$\text{Percent of Wound Area} = \frac{\text{Wound area}}{\text{Irradiated area}} \times 100\%$$

Histopathological Evaluation

Wound tissue samples were harvested from each wound, fixed in 4% paraformaldehyde, and embedded in paraffin wax following standard histological protocols. H&E staining and Masson's trichrome staining were performed to evaluate histopathological alterations. Tissue sections were subjected to light-microscopic observation. Collagen deposition was assessed by calculating the collagen volume fraction (CVF), defined as the ratio of collagen-stained area to total tissue area, with data expressed as percentage values. This systematic quantitative analysis enabled objective comparison of tissue repair dynamics across experimental groups.

Immunohistochemistry

Immunohistochemical staining was conducted to evaluate the expression of CD31, α-SMA, TNF-α, IL-1β, and IL-10, thereby assessing the effects of BMSCs-Exos on angiogenesis and inflammation in RISI. Formalin-fixed, paraffin-embedded skin sections were deparaffinized, rehydrated through a graded ethanol series, and subjected to antigen retrieval in 10 mM sodium citrate buffer (pH = 6.0) at 95 °C for 20 min. Subsequently, skin tissue slides were placed in antibody solution (primary antibodies, 4 °C, 16 h) for immunohistochemical staining: CD31 (1:4000, Proteintech, 28083-1-AP, Wuhan, China), *α*-SMA (1:3000, Proteintech, 14395-1-AP, Wuhan, China), TNF-α (1:400, Proteintech, 60291-1-1g, Wuhan, China), IL-10 (1:200, Proteintech, 60269-1-1g, Wuhan, China), IL-1β (1:300, bioss, bs-0812R, Beijing, China), following PBS washes, sections were incubated with an horseradish peroxidase (HRP)-conjugated secondary antibody. Visualization was achieved using 3,3′-diaminobenzidine (DAB) substrate, and nuclei were

counterstained with hematoxylin. Stained tissue sections were subjected to microscopic examination utilizing a light microscope, with representative images captured at 200× magnification.

Immunofluorescence

Paraffin-embedded skin sections for immunofluorescence staining were subjected to antigen retrieval using EDTA buffer (pH = 9.0) at 95 °C for 20 min to expose antigenic sites. Following retrieval, sections underwent fluorescence quenching with 0.1% sodium borohydride and membrane permeabilization with 0.3% Triton X-100 in PBS for 15 minutes each, with thorough washing between steps. To reduce background staining, tissue sections were incubated in 5% BSA/PBS for 1 hour at room temperature, followed by overnight primary antibody incubation at 4 ° C: CD86 (1:200, Bioss, bs-1035R, Beijing, China) as a marker for pro-inflammatory M1 macrophages, and CD206 (1:800, CST, 24595, USA) as a marker for anti-inflammatory M2 macrophages. Subsequent to a series of washes with PBS, sections were treated with an HRP-conjugated secondary antibody. Nuclear staining was achieved with DAPI for 10 min, after which samples were mounted in ProLong Gold antifade and imaged using a fluorescence microscope with suitable filter sets.

TUNEL Staining

Tissue samples were immersed in 4% paraformaldehyde (PFA) at 4 °C for 24 h to preserve cellular structures, followed by paraffin embedding and sectioning into 5-μm-thick slices. Deparaffinization with xylene and rehydration through graded ethanol was followed by thorough PBS washing. To block endogenous peroxidase activity, tissue sections were incubated in 3% hydrogen peroxide (H_2O_2) for 10 min at room temperature (RT), followed by three 5-min PBS washes to remove residual H_2O_2. Tissues were then treated with 100 μL of proteinase K working solution (20 μg/mL in 10 mM Tris-HCl, pH = 7.4) for 20 minutes at 37 °C to permeabilize cell membranes and expose DNA fragments. After additional PBS washing, sections were equilibrated with 100 μL TdT equilibrium buffer for 20 minutes at 37 °C. Following the removal of the equilibrium buffer, sections were incubated with 50 μL of TUNEL labeling solution at 37 °C for 60 min in the dark within a humidified chamber. After PBS rinsing, nuclear counterstaining was performed with DAPI for 5 min at room temperature, and slides were mounted for fluorescence microscopy.

Western Blotting

Skin tissue samples (100 mg) were homogenized in 1 mL RIPA lysis buffer to extract total protein. The protein concentration was determined using the BCA method, and 10% SDS-PAGE was performed to separate proteins, which were then transferred to a PVDF membrane. The membrane was blocked with 5% skim milk for 1 hour, followed by overnight incubation at 4 °C with the following primary

antibodies: *β*-actin (1:6000, Bioss, bs-0061R, Beijing, China), Arg-1 (1:1000, Wanlei, WL02825, Shenyang, China), iNOS (1:1000, Wanlei, WL0992a, Shenyang, China), Bax (1:2000, Proteintech, 50599-2-Ig, Wuhan, China), Bcl-2 (1:2000, Proteintech, 26593-1-AP, Wuhan, China), *p*-Akt (1:2000, Proteintech, 28731-1-AP, Wuhan, China), Akt (1:2000, Proteintech, 10176-2-AP, Wuhan, China). Following PBS washes, membranes were incubated with HRP-conjugated secondary antibodies at room temperature for 1 h. Signals visualized through a reaction with an optimized enhanced chemiluminescence (ECL) substrate, captured using a gel imaging system, and quantified with ImageJ software.

Statistical Analysis

Statistical analyses were performed using SPSS software (version 23.0) and GraphPad Prism (version 10.0). Quantitative data are presented as mean ± standard deviation ($\bar{x} \pm s$) unless otherwise specified. One-way ANOVA was employed to assess whether there were significant differences among the means of multiple groups, followed by an LSD-t post hoc test for pairwise comparisons. For non-parametric data, the Kruskal-Wallis H test was employed for overall comparisons, followed by the Mann-Whitney U test for pairwise analyses. Statistical significance was set at $P < 0.05$.

Conclusions

In summary, this study demonstrates the therapeutic potential of BMSCs-Exos in treating radiation-induced skin injury (RISI). BMSCs-Exos effectively reduced the injury area and severity, while promoting tissue repair and accelerating wound healing. The therapeutic effects of BMSCs-Exos are primarily mediated through the modulation of inflammation and the inhibition of apoptosis in irradiated tissues. These findings suggest that BMSCs-Exos could be a promising novel approach for RISI treatment.

Acknowledgments: The authors would like to thank Xu Tong for their valuable contributions to the study design and manuscript revisions. We also appreciate the Qiqihar Medical University for offering the experimental animals. Special thanks to all animals involved in the study.

Author Contributions: Yuxin Wen and Xu Tong conceptualized the study; Shichao Pan and Na Zhang developed the methodology; Yuxin Wen and Yiwei Song performed the experiments and collected the data; Yuxin Wen analyzed the data and drafted the manuscript; Xu Tong and Shichao Pan reviewed and edited the manuscript. All authors reviewed and approved the final version of the paper.

Funding: This research was supported by the Joint Fund Cultivation Project of Heilongjiang Provincial Natural Science Foundation (PL2024H261), the Qiqihar Medical University

Graduate Innovation Fund (QYYCX2023-12), and the Construction Project of Dominant Characteristic Disciplines of Qiqihar Medical University (QYZDXK-025, Oncology).

Data Availability: The data used to support the findings of this study are available from the corresponding author upon request.

Code Availability: Not applicable.

Declarations

Ethics Approval and Consent to Participate: All experimental procedures and animal experiments were approved by the Animal Ethics Committee of Qiqihar Medical University, with approval number QMU-AECC-2024-7.

Consent for Publication: All authors consented to publish this paper.

Competing Interests: All authors declared that there is no confict of interest.

Clinical trial number: Not applicable.

References

1. Singh, M., Alavi, A., Wong, R., & Akita, S. (2016). Radiodermatitis: A review of our current understanding. *American journal of clinical dermatology*, *17*(3), 277-292.
2. Wong, R. K., Bensadoun, R. J., Boers-Doets, C. B., Bryce, J., Chan, A., Epstein, J. B., Eaby-Sandy, B., & Lacouture, M. E. (2013). Clinical practice guidelines for the prevention and treatment of acute and late radiation reactions from the MASCC skin toxicity study group. *Supportive care in cancer : official journal of the Multinational Association of Supportive Care in Cancer*, *21*(10), 2933-2948.
3. Najafi, M., Motevaseli, E., Shirazi, A., Geraily, G., Rezaeyan, A., Norouzi, F., Rezapoor, S., & Abdollahi, H. (2018). Mechanisms of inflammatory responses to radiation and normal tissues toxicity: Clinical implications. *International journal of radiation biology*, *94*(4), 335-356.
4. Zhou, L., Zhu, J., Liu, Y., Zhou, P. K., & Gu, Y. (2024). Mechanisms of radiation-induced tissue damage and response. *MedComm*, *5*(10), e725.
5. Feng, Z., Zhang, Y., Yang, C., Liu, X., Huangfu, Y., Zhang, C., Huang, P., Dong, A., Liu, J., Liu, J., Kong, D., & Wang, W. (2023). Bioinspired and inflammation-modulatory glycopeptide hydrogels for radiation-induced chronic skin injury repair. *Advanced healthcare materials*, *12*(1), e2201671.
6. Zhang, Y., Zhang, S., & Shao, X. (2013). Topical agent therapy for prevention and treatment of radiodermatitis: a meta-analysis. *Supportive*

care in cancer : official journal of the Multinational Association of Supportive Care in Cancer, *21*(4), 1025-1031.

7. Sun, J., Shi, C. S., & Wang, D. L. (2021). [Research advances on the roles of exosomes derived from mesenchymal stem cells in wound healing and prevention and treatment of hypertrophic scars]. *Zhonghua shao shang za zhi = Zhonghua shaoshang zazhi = Chinese journal of burns*, *37*(5), 495-500.
8. Caplan, H., Olson, S. D., Kumar, A., George, M., Prabhakara, K. S., Wenzel, P., Bedi, S., Toledano-Furman, N. E., Triolo, F., Kamhieh-Milz, J., Moll, G., & Cox, C. S. Jr. (2019). Mesenchymal Stromal Cell Therapeutic Delivery: Translational Challenges to Clinical Application. *Frontiers in immunology*, *10*, 1645.
9. Sissung, T. M., & Figg, W. D. (2020). Stem cell clinics: risk of proliferation. *The Lancet. Oncology*, *21*(2), 205-206.
10. Qin, X., He, J., Wang, X., Wang, J., Yang, R., & Chen, X. (2023). The functions and clinical application potential of exosomes derived from mesenchymal stem cells on wound repair: a review of recent research advances. *Frontiers in immunology*, *14*, 1256687.
11. Boilard, E. (2018). Extracellular vesicles and their content in bioactive lipid mediators: More than a sack of microRNA. *Journal of lipid research*, *59*(11), 2037-2046.
12. Kalluri, R., & LeBleu, V. S. (2020). The biology, function, and biomedical applications of exosomes. *Science*, *367*(6478), eaau6977.
13. Liu, J., Yan, Z., Yang, F., Huang, Y., Yu, Y., Zhou, L., Sun, Z., Cui, D., & Yan, Y. (2021). Exosomes Derived from Human Umbilical Cord Mesenchymal Stem Cells Accelerate Cutaneous Wound Healing by Enhancing Angiogenesis through Delivering Angiopoietin-2. *Stem cell reviews and reports*, *17*(2), 305-317.
14. Niu, Q., Yang, Y., Li, D., Guo, W., Wang, C., Xu, H., Feng, Z., & Han, Z. (2022). Exosomes derived from bone marrow mesenchymal stem cells alleviate ischemia-reperfusion injury and promote survival of skin flaps in rats. *Life (Basel, Switzerland)*, *12*(10), 1567.
15. Xu, R., Zhang, F., Chai, R., Zhou, W., Hu, M., Liu, B., Chen, X., Liu, M., Xu, Q., Liu, N., & Liu, S. (2019). Exosomes derived from pro-inflammatory bone marrow-derived mesenchymal stem cells reduce inflammation and myocardial injury via mediating macrophage polarization. *Journal of cellular and molecular medicine*, *23*(11), 7617-7631.
16. Tang, T., Chen, L., Zhang, M., Wang, C., Du, X., Ye, S., Li, X., Chen, H., & Hu, N. (2024). Exosomes derived from BMSCs enhance diabetic wound healing through circ-Snhg11 delivery. *Diabetology & metabolic syndrome*, *16*(1), 37.
17. Huang, C., Lu, G., Jia, Z., & Yan, J. (2025). Mesenchymal Stem Cell-Derived Exosome miR-153-3 Induced M2-Type Polarization of Macrophages to

Improve the Healing Effect of Burn Wounds. *Applied biochemistry and biotechnology*, *197*(6), 3841-3855.

18. Shen, C., Tao, C., Zhang, A., Li, X., Guo, Y., Wei, H., Yin, Q., Li, Q., & Jin, P. (2022). Exosomal microRNA□93□3p secreted by bone marrow mesenchymal stem cells downregulates apoptotic peptidase activating factor 1 to promote wound healing. *Bioengineered*, *13*(1), 27-37.
19. Hegedus, F., Mathew, L. M., & Schwartz, R. A. (2017). Radiation dermatitis: an overview. *International journal of dermatology*, *56*(9), 909-914.
20. Brown, K. R., & Rzucidlo, E. (2011). Acute and chronic radiation injury. *Journal of vascular surgery*, *53*(1 Suppl), 15S-21S.
21. Morton, L. M., & Phillips, T. J. (2016). Wound healing and treating wounds: Differential diagnosis and evaluation of chronic wounds. *Journal of the American Academy of Dermatology*, *74*(4), 589-605; quiz 605-606.
22. Wei, J., Meng, L., Hou, X., Qu, C., Wang, B., Xin, Y., & Jiang, X. (2019). Radiation-induced skin reactions: mechanism and treatment. *Cancer management and research*, *11*, 167-177.
23. Yang, X., Ren, H., Guo, X., Hu, C., & Fu, J. (2020). Radiation-induced skin injury: pathogenesis, treatment, and management. *Aging*, *12*(22), 23379-23393.
24. Hu, J. C., Zheng, C. X., Sui, B. D., Liu, W. J., & Jin, Y. (2022). Mesenchymal stem cell-derived exosomes: A novel and potential remedy for cutaneous wound healing and regeneration. *World journal of stem cells*, *14*(5), 318-329.
25. Manchon, E., Hirt, N., Bouaziz, J. D., Jabrane-Ferrat, N., & Al-Daccak, R. (2021). Stem cells-derived extracellular vesicles: Potential therapeutics for wound healing in chronic inflammatory skin diseases. *International journal of molecular sciences*, *22*(6), 3130.
26. Zhou, C., Zhang, B., Yang, Y., Jiang, Q., Li, T., Gong, J., Tang, H., & Zhang, Q. (2023). Stem cell-derived exosomes: Emerging therapeutic opportunities for wound healing. *Stem cell research & therapy*, *14*(1), 107.
27. Avadanei-Luca, S., Nacu, I., Avadanei, A. N., Pertea, M., Tamba, B., Verestiuc, L., & Scripcariu, V. (2025). Tissue Regeneration of Radiation-Induced Skin Damages Using Protein/Polysaccharide-Based Bioengineered Scaffolds and Adipose-Derived Stem Cells: A Review. *International journal of molecular sciences*, *26*(13), 6469.
28. Yang, E. H., Marmagkiolis, K., Balanescu, D. V., Hakeem, A., Donisan, T., Finch, W., Virmani, R., Herrman, J., Cilingiroglu, M., Grines, C. L., Toutouzas, K., & Iliescu, C. (2021). Radiation-Induced Vascular Disease-A State-of-the-Art Review. *Frontiers in cardiovascular medicine*, *8*, 652761.
29. Li, F. Q., Chen, W. B., Luo, Z. W., Chen, Y. S., Sun, Y. Y., Su, X. P., Sun, J. M., & Chen, S. Y. (2023). Bone marrow mesenchymal stem cell-derived

exosomal microRNAs target PI3K/Akt signaling pathway to promote the activation of fibroblasts. *World journal of stem cells*, *15*(4), 248-267.

30. Li, B., Luan, S., Chen, J., Zhou, Y., Wang, T., Li, Z., Fu, Y., Zhai, A., & Bi, C. (2020). The MSC-Derived Exosomal lncRNA H19 Promotes Wound Healing in Diabetic Foot Ulcers by Upregulating PTEN via MicroRNA-152-3p. *Molecular therapy. Nucleic acids*, *19*, 814-826.
31. Jiang, T., Wang, Z., & Sun, J. (2020). Human bone marrow mesenchymal stem cell-derived exosomes stimulate cutaneous wound healing mediates through TGF-β/Smad signaling pathway. *Stem cell research & therapy*, *11*(1), 198.
32. Simman, R., Bach, K., Abbas, F., Klomparens, K., & Brickman, B. J. (2023). Management of Radiation-induced Tissue Injuries: A Review of Current Treatment Strategies. *Plastic and reconstructive surgery. Global open*, *11*(6), e5043.
33. Oishi, Y., & Manabe, I. (2018). Macrophages in inflammation, repair and regeneration. *International immunology*, *30*(11), 511-528.
34. Wynn, T. A., & Vannella, K. M. (2016). Macrophages in Tissue Repair, Regeneration, and Fibrosis. *Immunity*, *44*(3), 450-462.
35. Hu, M. S., Walmsley, G. G., Barnes, L. A., Weiskopf, K., Rennert, R. C., Duscher, D., Januszyk, M., Maan, Z. N., Hong, W. X., Cheung, A. T., Leavitt, T., Marshall, C. D., Ransom, R. C., Malhotra, S., Moore, A. L., Rajadas, J., Lorenz, H. P., Weissman, I. L., Gurtner, G. C., & Longaker, M. T. (2017). Delivery of monocyte lineage cells in a biomimetic scaffold enhances tissue repair. *JCI insight*, *2*(19), e96260.
36. Kim, H., Wang, S. Y., Kwak, G., Yang, Y., Kwon, I. C., & Kim, S. H. (2019). Exosome-guided phenotypic switch of M1 to M2 macrophages for cutaneous wound healing. *Advanced science (Weinheim, Baden-Wurttemberg, Germany)*, *6*(20), 1900513.
37. Geng, X., Qi, Y., Liu, X., Shi, Y., Li, H., & Zhao, L. (2022). A multifunctional antibacterial and self-healing hydrogel laden with bone marrow mesenchymal stem cell-derived exosomes for accelerating diabetic wound healing. *Biomaterials Advances*, *133*, 112613.
38. Arabpour, M., Saghazadeh, A., & Rezaei, N. (2021). Anti-inflammatory and M2 macrophage polarization-promoting effect of mesenchymal stem cell-derived exosomes. *International immunopharmacology*, *97*, 107823.
39. Deng, H., Wu, L., Liu, M., Zhu, L., Chen, Y., Zhou, H., Shi, X., Wei, J., Zheng, L., Hu, X., Wang, M., He, Z., Lv, X., & Yang, H. (2020). Bone marrow mesenchymal stem cell-derived exosomes attenuate LPS-induced ARDS by modulating macrophage polarization through inhibiting glycolysis in macrophages. *Shock*, *54*(6), 828-843.
40. Chang, Q., Hao, Y., Wang, Y., Zhou, Y., Zhuo, H., & Zhao, G. (2021). Bone marrow mesenchymal stem cell-derived exosomal microRNA-125a

promotes M2 macrophage polarization in spinal cord injury by downregulating IRF5. *Brain research bulletin*, *170*, 199-210.

41. Li, R., Zhao, K., Ruan, Q., Meng, C., & Yin, F. (2020). Bone marrow mesenchymal stem cell-derived exosomal microRNA-124-3p attenuates neurological damage in spinal cord ischemia-reperfusion injury by downregulating Ern1 and promoting M2 macrophage polarization. *Arthritis research & therapy*, *22*(1), 75.
42. Liu, C., Wei, J., Wang, X., Zhao, Q., Lv, J., Tan, Z., Xin, Y., & Jiang, X. (2024). Radiation-induced skin reactions: Oxidative damage mechanism and antioxidant protection. *Frontiers in cell and developmental biology*, *12*, 1480571.
43. Zhou, H., Li, X. M., Meinkoth, J., & Pittman, R. N. (2000). Akt regulates cell survival and apoptosis at a postmitochondrial level. *The Journal of cell biology*, *151*(3), 483-494.
44. Xu, Y. C., Lin, Y. S., Zhang, L., Lu, Y., Sun, Y. L., Fang, Z. G., Li, Z. Y., & Fan, R. F. (2020). MicroRNAs of bone marrow mesenchymal stem cell-derived exosomes regulate acute myeloid leukemia cell proliferation and apoptosis. *Chinese medical journal*, *133*(23), 2829-2839.
45. Scuteri, A., Donzelli, E., Foudah, D., Caldara, C., Redondo, J., D'Amico, G., Tredici, G., & Miloso, M. (2014). Mesengenic differentiation: comparison of human and rat bone marrow mesenchymal stem cells. *International journal of stem cells*, *7*(2), 127-134.
46. Douglas, B. G., & Fowler, J. F. (2012). The effect of multiple small doses of X rays on skin reactions in the mouse and a basic interpretation. 1976. *Radiation research*, *178*(2), AV125-138.

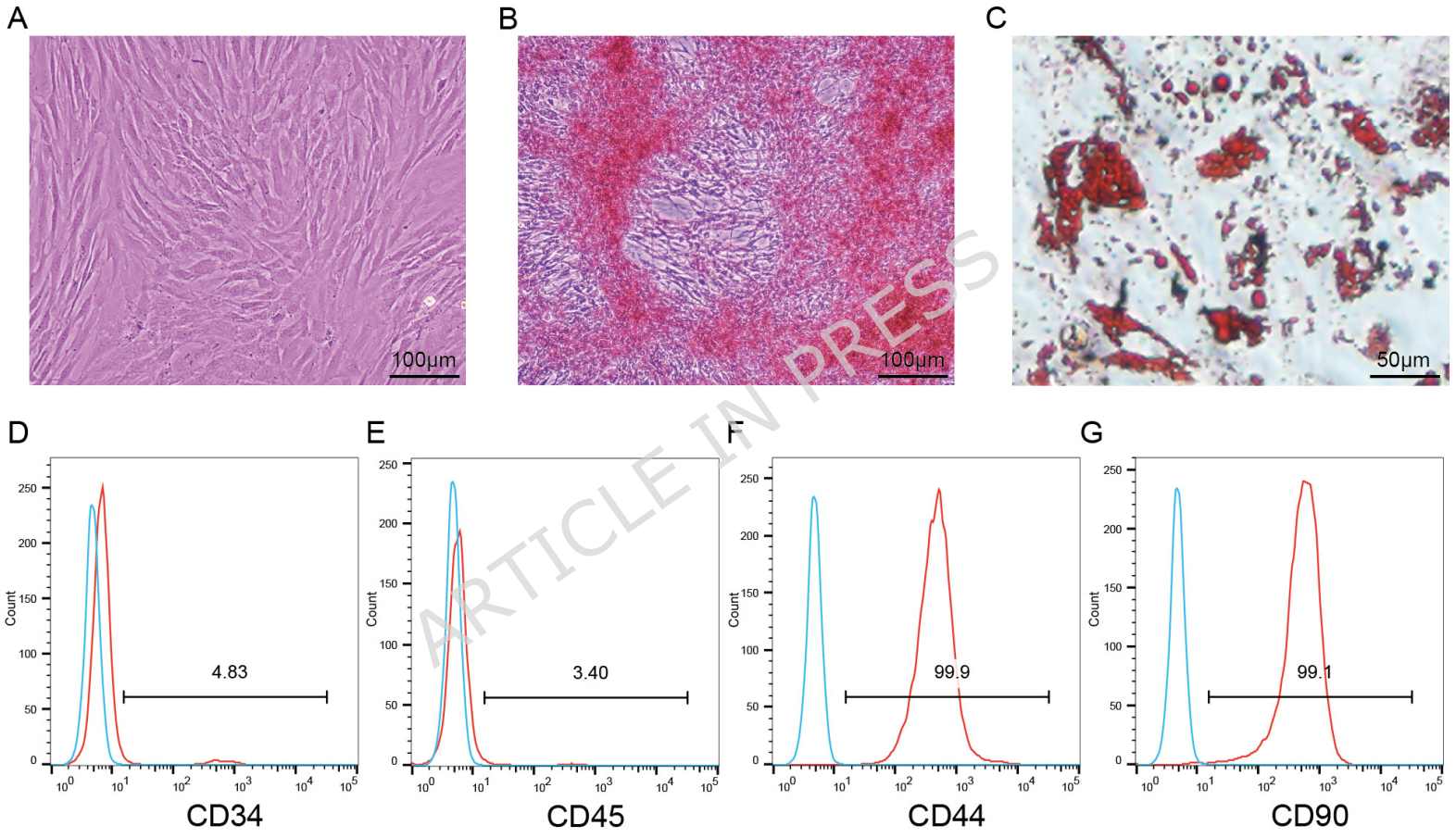

A

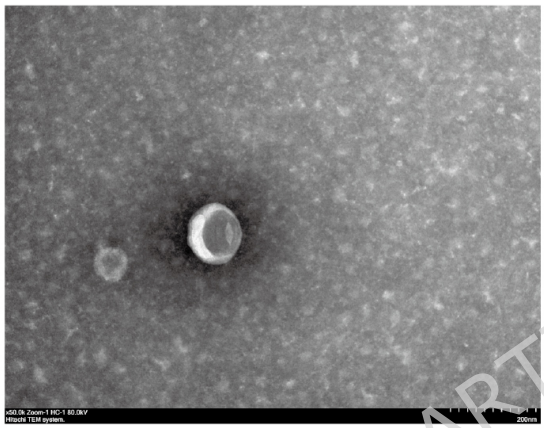

B

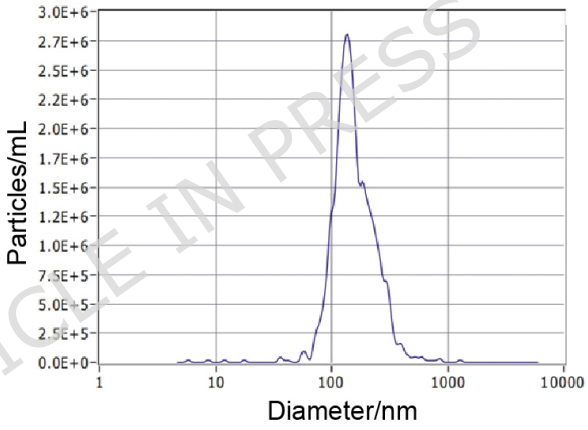

C

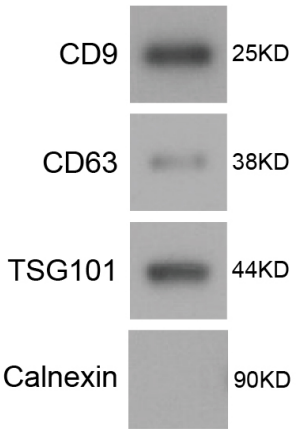

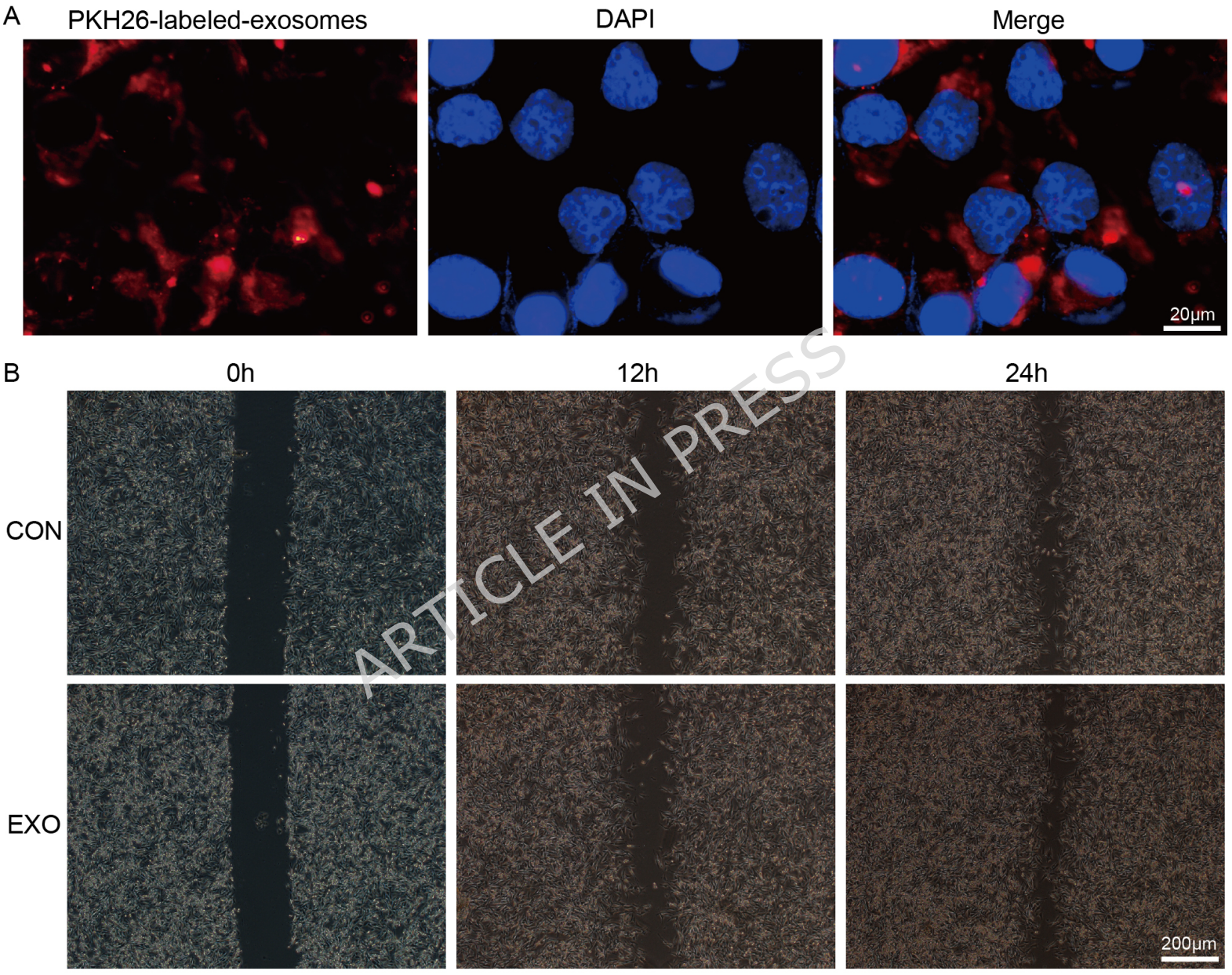

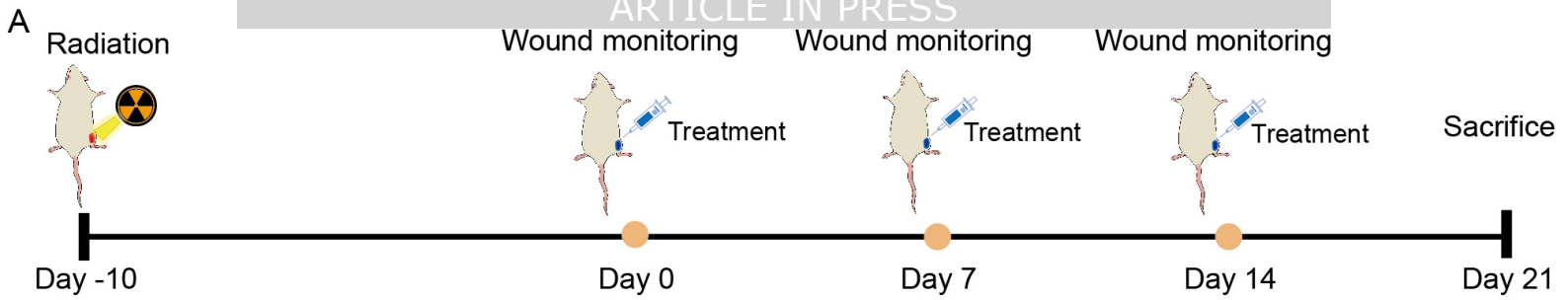

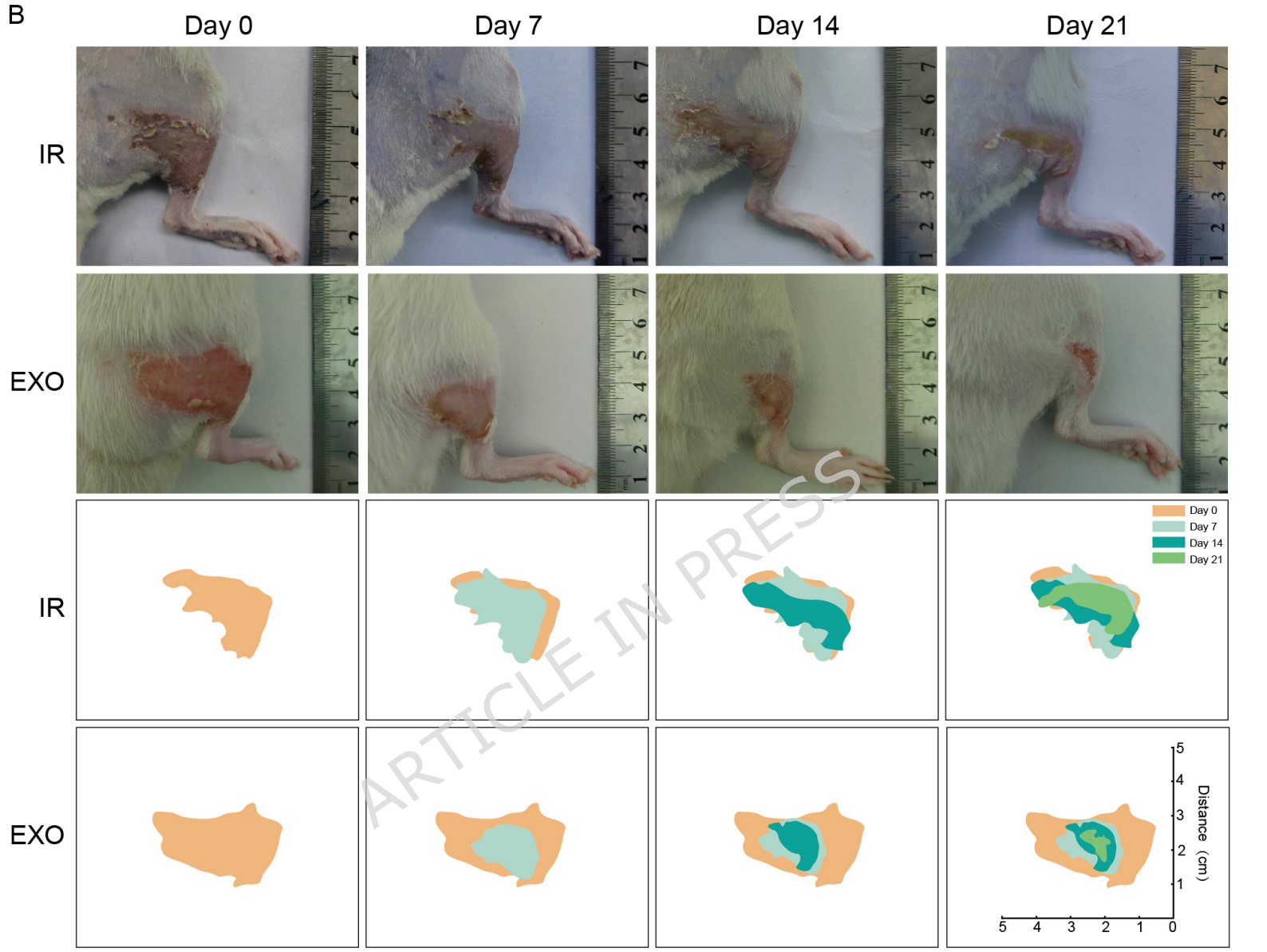

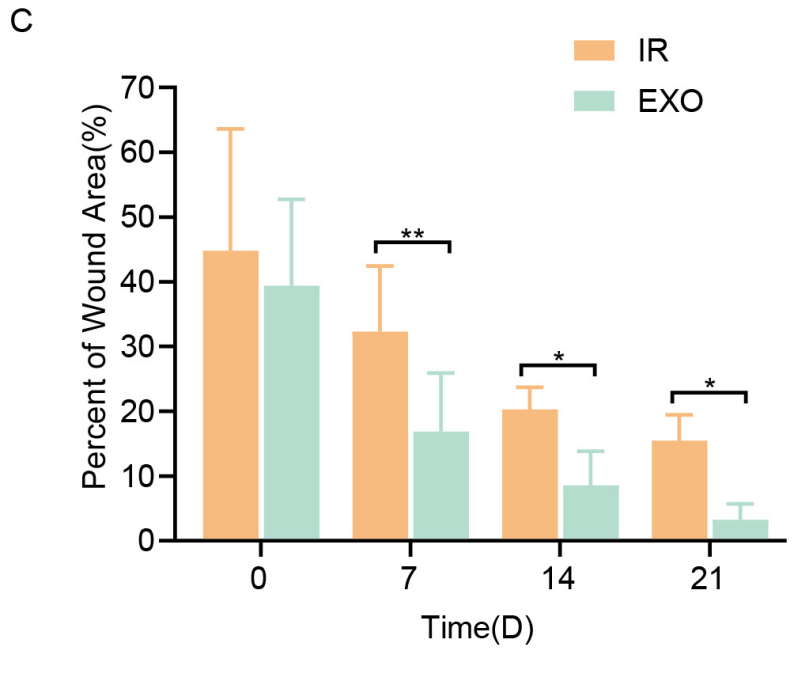

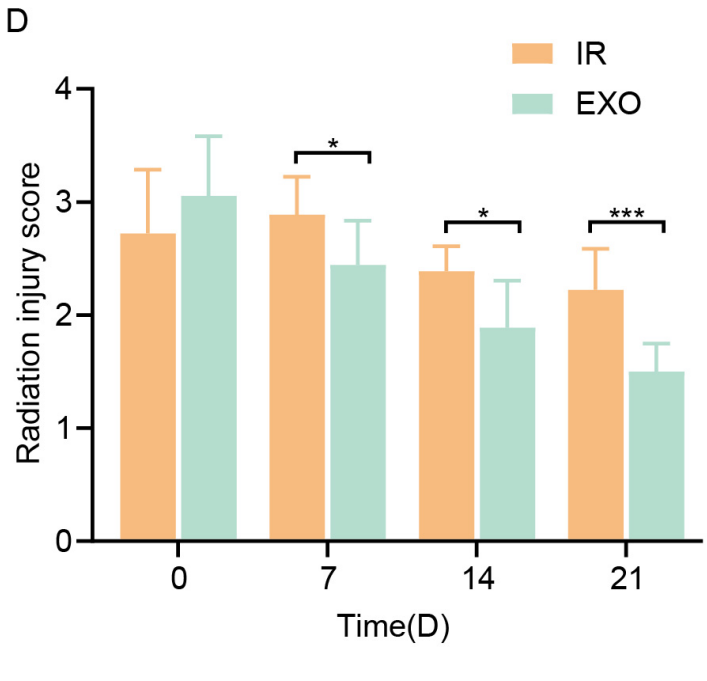

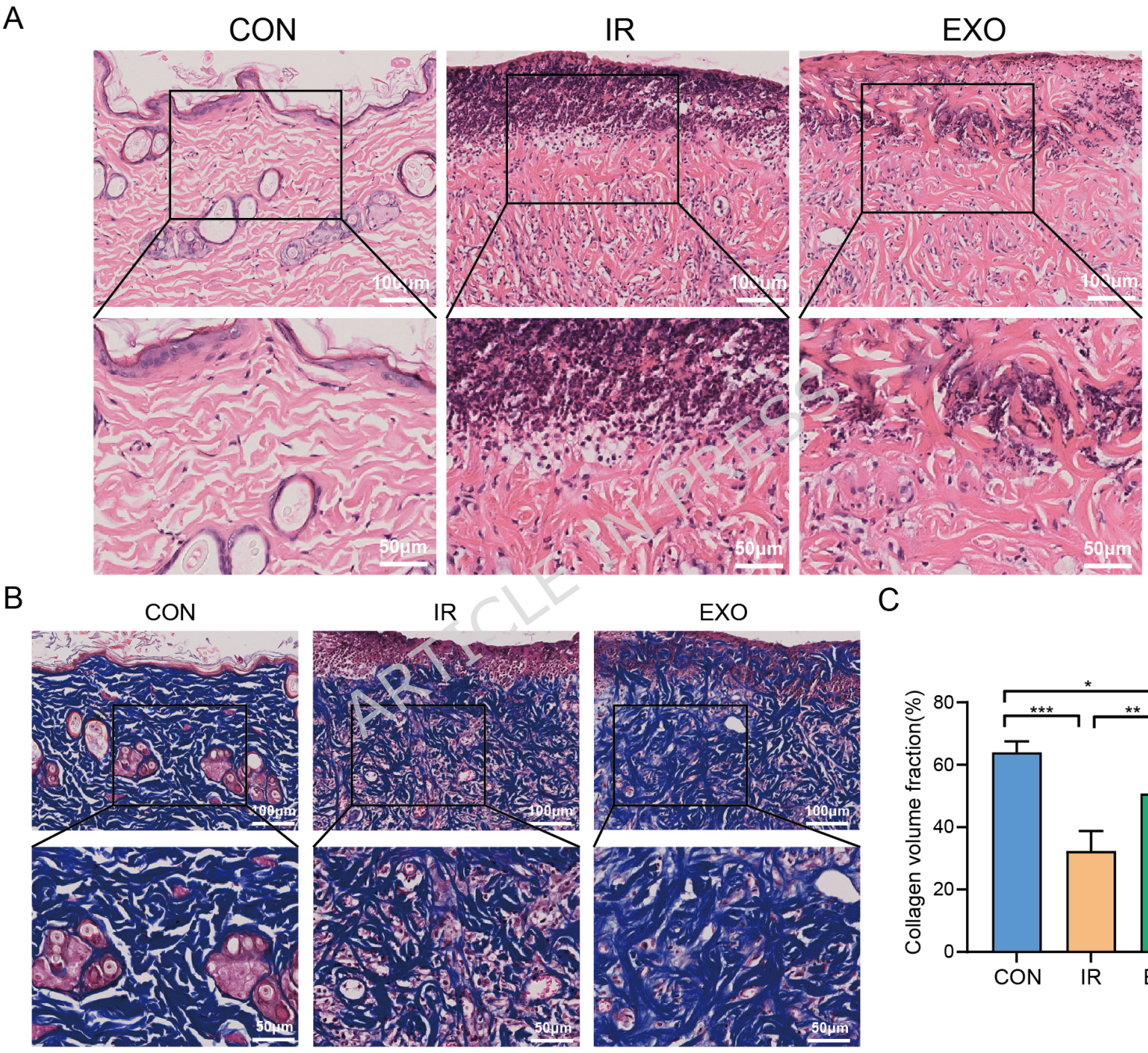

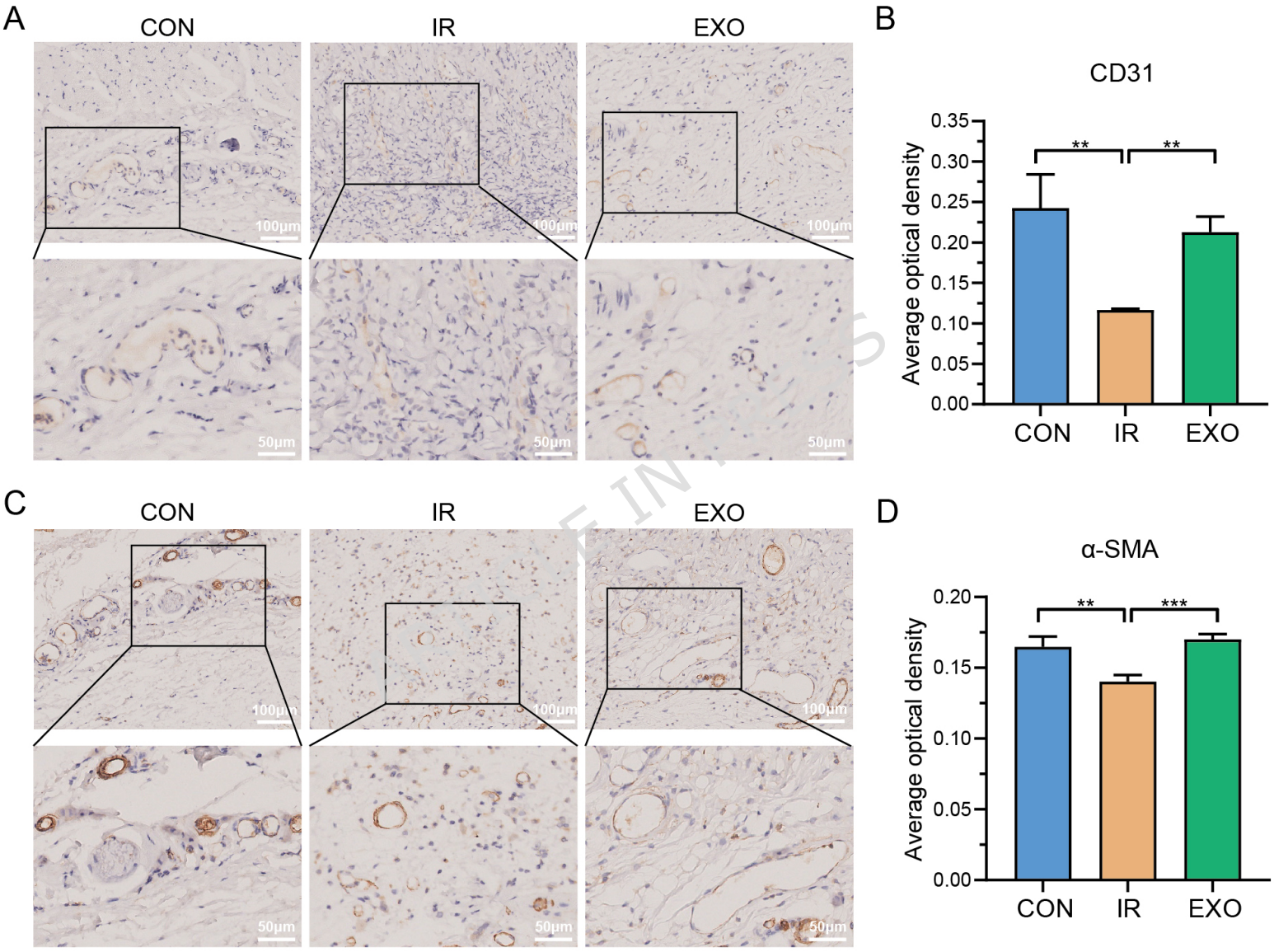

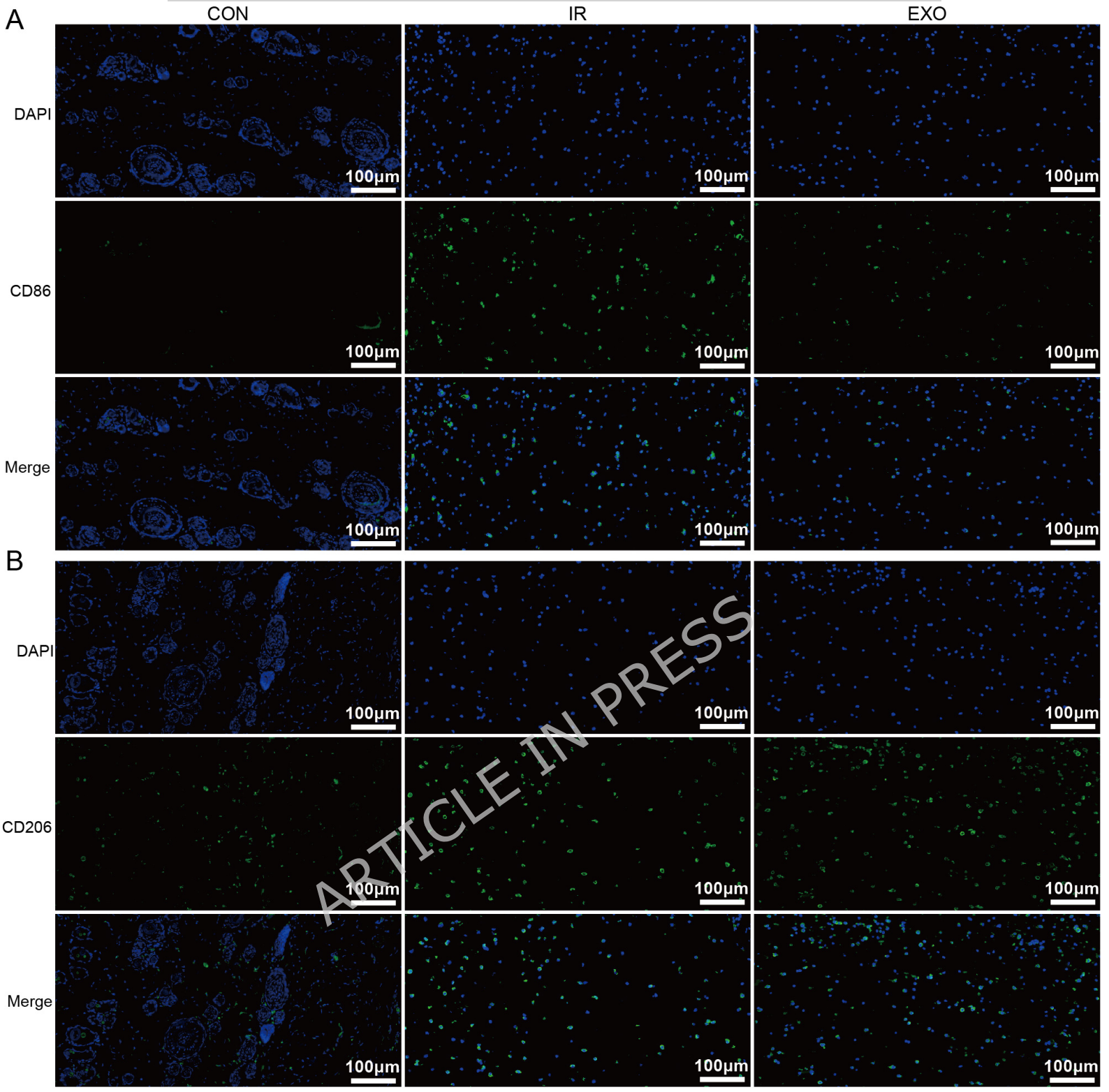

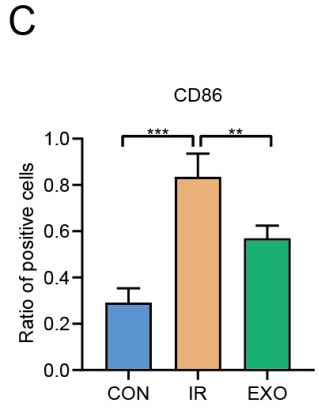

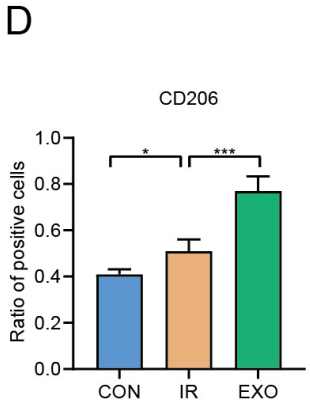

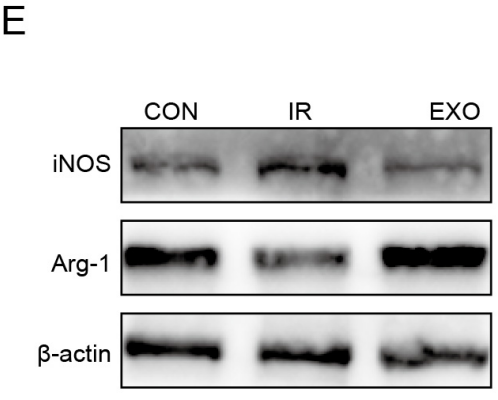

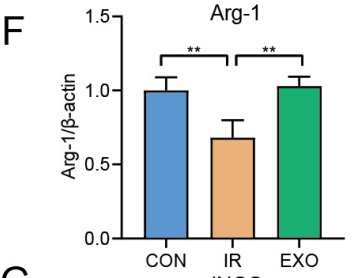

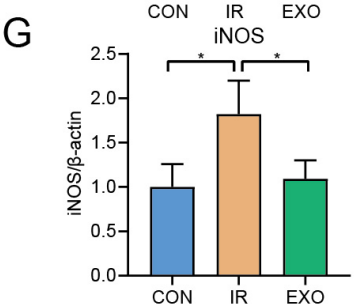

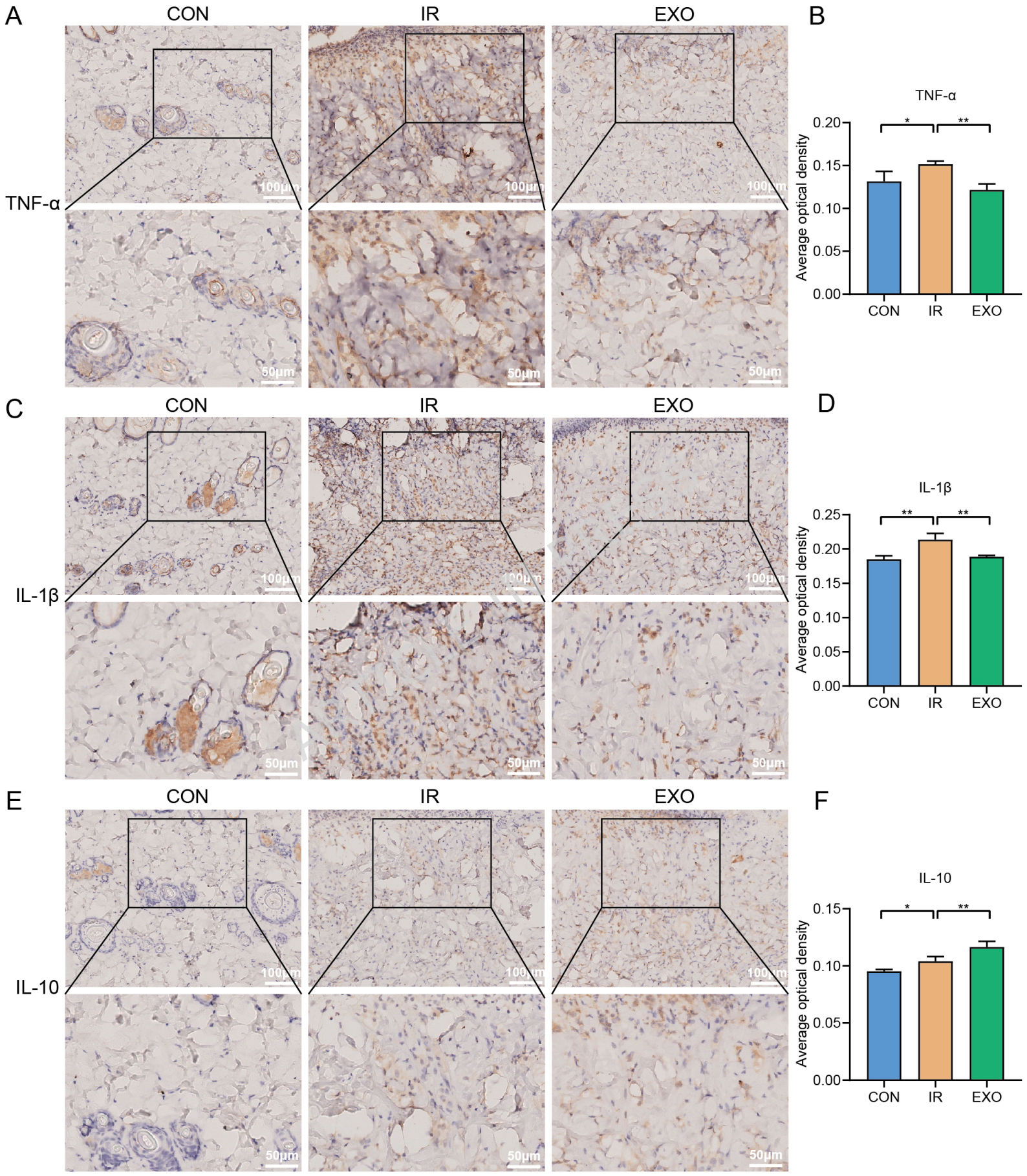
A
CON
IR
EXO
TNF-α
100μm
50μm
B
TNF-α
Average optical density
0.20
0.15
0.10
0.05
0.00
*
**
CON
IR
EXO
C
CON
IR
EXO
IL-1β
100μm
50μm
D
IL-1β
Average optical density
0.25
0.20
0.15
0.10
0.05
0.00
**
**
CON
IR
EXO
E
CON
IR
EXO
IL-10
100μm
50μm
F
IL-10
Average optical density
0.15
0.10
0.05
0.00
*
**
CON
IR
EXO